

1 **Ground-level gaseous pollutants (NO₂, SO₂, and CO)**
2 **acrossin China: daily seamless mapping and ~~long-term~~**
3 **spatiotemporal variations**

4
5 Jing Wei^{1*}, Zhanqing Li^{1*}, Jun Wang², Can Li¹, Pawan Gupta^{3,4}, Maureen Cribb¹
6

7 1. Department of Atmospheric and Oceanic Science, Earth System Science Interdisciplinary
8 Center, University of Maryland, College Park, MD, USA

9 2. Department of Chemical and Biochemical Engineering, Iowa Technology Institute, Center for
10 Global and Regional Environmental Research, University of Iowa, USA

11 3. STI, Universities Space Research Association (USRA), Huntsville, AL, USA

12 4. NASA Marshall Space Flight Center, Huntsville, AL, USA
13

14 * Correspondence: Zhanqing Li (zhanqing@umd.edu); Jing Wei (weijing@umd.edu)
15

16 **Abstract**

17 Gaseous pollutants at the ground level seriously threaten the urban air quality environment and
18 public health. There are few estimates of gaseous pollutants that are spatially and temporally
19 resolved and continuous ~~over long periods in across~~ China. This study takes advantage of big data
20 and artificial intelligence technologies to generate seamless daily maps of three major ambient
21 pollutant gases, i.e., NO₂, SO₂, and CO, across China from 2013 to 2020 at a uniform spatial
22 resolution of 10 km. Cross-validation between our estimates and ground observations illustrated a
23 high data quality on a daily basis for surface NO₂, SO₂, and CO concentrations, with mean ~~out-of-~~
24 ~~bag~~ coefficients of determination (root-mean-square errors) of 0.84 (7.99 μg/m³), 0.84 (10.7 μg/m³),
25 and 0.80 (0.29 mg/m³), respectively. ~~They have experienced significant declines and then recoveries~~
26 ~~during and after the~~ We found that the COVID-19 lockdown ~~associated with changes in~~
27 ~~anthropogenic emissions in eastern China, while surface CO recovered faster than SO₂ and NO₂.~~
28 ~~All had sustained impacts on~~ gaseous pollutants ~~decreased significantly by 0.23, 2.01, and 49 μg/m³~~
29 ~~per year (p < 0.001) across China during 2013–2020, especially in three urban agglomerations,~~
30 ~~where surface CO recovered to its normal level in China on around the 34th day after the Lunar New~~
31 ~~Year, while surface SO₂ and NO₂ rebounded more than twice slower due to more CO emissions~~
32 ~~from increased residents' indoor cooking and atmospheric oxidation capacity. Surface NO₂, SO₂,~~
33 ~~and CO reached their peak annual concentrations of 21.3 ± 8.8 μg/m³, 23.1 ± 13.3 μg/m³, and 1.01~~
34 ~~± 0.29 mg/m³ in 2013, then continuously declined over time by 12%, 55%, and 17%, respectively,~~
35 ~~until 2020.~~ The declining rates were ~~larger during~~ more prominent from 2013– to 2017 due to the
36 sharper reductions in anthropogenic emissions but have slowed down in recent years. ~~Both the areas~~
37 ~~and occurrence probabilities of days exceeding~~ Nevertheless, people still suffer from high-frequency
38 risk exposure to surface NO₂ in eastern China, while surface SO₂ and CO have almost reached the
39 recommended air quality guidelines level since 2018, benefiting from the implemented stricter
40 “ultra-low” emission standards ~~also gradually shrank and weakened over time, especially for SO₂~~
41 ~~and CO, which almost disappeared during 2018–2020, suggesting significant improvements in air~~
42 ~~quality in China.~~ This reconstructed dataset of surface gaseous pollutants, ~~i.e., ChinaHighNO₂,~~
43 ~~ChinaHighSO₂, and ChinaHighCO,~~ will benefit future (especially short-term) air pollution and
44 environmental health-related studies.

45

46 1. Introduction

47 Air pollution has been a major environmental concern, affecting human health, weather, and climate
48 (~~Kan et al., 2012~~; Kinney, 2008; ~~Li et al., 2017b~~; ~~Anenberg et al., 2022~~; Sun et al., 2010; ~~Kan et al.,~~
49 ~~2012~~; ~~Z. Li et al., 2017~~; ~~Murray et al., 2020~~; Orellano et al., ~~2020~~; ~~Murray et al., 2020~~; ~~Anenberg et~~
50 ~~al., 2022~~), and has thus ~~drawn~~ drawing worldwide attention. The sources of air pollution are
51 complex. They include natural sources such as wildfires and anthropogenic emissions, including
52 pollutants discharged from industrial production ([e.g., smoke/dust, sulfur oxides, nitrogen oxides
53 (NO_x), and volatile organic compounds (VOCs)], hazardous substances released from burning
54 coal during heating seasons ([e.g., dust, sulfur dioxide (SO₂), and carbon monoxide (CO)], and
55 waste gases (e.g., CO, SO₂, and NO_x) generated by transportation, especially in big cities.
56 Among various air pollutants, the ~~followings~~ following have been most widely recognized:
57 particulate ~~matters~~ (e.g., matter with diameters smaller than 2.5 μm and 10 μm (PM_{2.5} and PM₁₀)),
58 and gaseous pollutants ([e.g., ozone (O₃), nitrogen dioxide (NO₂), SO₂, and CO, among others].
59 Many countries have built ground-based networks to monitor a variety of conventional pollutants in
60 real-time. China has experienced serious ambient air pollution for a long time, prompting the
61 establishment of a large-scale air quality monitoring network (~~Mee, 2018~~), (~~MEE, 2018a~~). Over the
62 years, much effort has been made to model different species of air pollutants. Many studies focused
63 on particulate matter (e.g., PM₁, PM_{2.5}, and PM₁₀) in China have been carried out ~~with a focus on~~
64 ~~China~~ (~~Ma et al., 2022~~; Fang et al., 2016; ~~Wei T. Li et al., 2019b~~; ~~2017~~; ~~G. Chen et al., 2018~~; ~~Wei et~~
65 ~~al., 2021a~~; ~~Wei et al., 2021b~~; ~~Li et al., 2017a~~; ~~Z. Zhang et al., 2018~~; ~~Ma et al., 2022~~). The global
66 COVID-19 pandemic has motivated many attempts to estimate surface NO₂ concentrations (~~Tian et~~
67 ~~al., 2020~~; ~~Who, 2020~~) ~~from various~~ from satellite-retrieved tropospheric NO₂ products, e.g., ~~OMI~~
68 ~~and~~ (Tian et al., 2020; WHO, 2020), e.g., from the Ozone Monitoring Instrument (OMI) onboard
69 the NASA Aura spacecraft and the TROPOspheric Monitoring Instrument (TROPOMI, by) onboard
70 the Copernicus Sentinel-5 Precursor satellite, adopting different statistical regression (~~Chi et al.,~~
71 ~~2021~~; Qin et al., 2017; ~~Z. Zhang et al., 2018~~; ~~Chi et al., 2021~~) and artificial intelligence (~~Chi et al.,~~
72 ~~2022~~; ~~Dou et al., 2021~~; ~~Chen et al., 2019~~; Zhan et al., 2018; ~~Z.-Y. Chen et al., 2019~~; ~~Dou et al.,~~
73 ~~2021~~; ~~Liu, 2021~~; ~~Y. Wang et al., 2021~~; ~~Liu, 2021~~ ~~Chi et al., 2022~~) models. ~~In contrast, studies on~~
74 comparison, surface SO₂ and CO ~~with a focus on whole of~~ in China are ~~meager~~ less studied, limited

75 by weaker signals and a lack of good-quality satellite tropospheric ~~satellite remote sensing~~ products
76 ~~and weaker signals~~ (Li et al., 2020; D. Liu et al., 2019; R. Li et al., 2020; Y. Wang et al., 2021; W.
77 Han et al., 2022, 2022b). Such studies still face more challenges, e.g., satellite data gaps and missing
78 values that seriously limit their application and the neglect of ~~the spatial and~~
79 ~~temporal~~ spatiotemporal differences in air pollution in the modeling process. In addition, most
80 previous studies mainly focused on studying a single or a few species during relatively short
81 observational periods ~~of observation~~.

82 ~~As such, here, we aim~~ In view of the above problems, the purpose of this paper is to reconstruct a
83 ~~long-term~~ daily seamless dataset concentrations of three ambient gaseous pollutants (i.e., surface
84 NO₂, SO₂, and CO) in China. To this end, relying on the dense national ground-based observation
85 network and big data, including satellite remote sensing products, meteorological reanalysis,
86 chemical model simulations, and emission inventories, we are capable of mapping three pollutant
87 gases seamlessly (100% spatial coverage) on a daily basis at a uniform 10 km spatial resolution to
88 study air quality. We adopted the spatiotemporal ensemble of 10 km since 2013 in China. Estimates
89 were made using an extended and powerful machine-learning model to estimate three surface
90 gaseous pollutants from big data, incorporating spatiotemporal information, i.e., space-time extra-
91 trees. Natural and anthropogenic effects on air pollution, including their physical mechanisms and
92 chemical reactions, were accounted for in the modeling. Using this dataset, ~~the long-term~~
93 spatiotemporal variations of the ~~three~~ gaseous pollutants ~~and~~, the impacts of implementing
94 environmental protection policies and the COVID-19 epidemic, and population risk exposure to
95 gaseous pollution are investigated.

96 To date, we have combined the advantages of artificial intelligence and big data to construct a
97 virtually complete set of major air quality parameters concerning both particulate and gaseous
98 pollutants over a long period of time across China, including PM₁ (2000–Present, Wei et al., 2019),
99 PM_{2.5} (2000–Present, Wei et al., 2020; Wei et al., 2021a), PM₁₀ (2000–Present, Wei et al., 2021b),
100 O₃ (1979–Present, Wei et al., 2022a; He et al., 2022), and NO₂ (2019–Present, Wei et al., 2022b),
101 servicing environmental, public health, economy, and other related research. This study is the
102 continuation of our previous studies, which adds two new species of SO₂ and CO for the first time
103 and also dates the data records of NO₂ back to 2013. Instead of devoting itself to a single pollutant,

104 this study deals with all gaseous pollutants of compatible quality over the same period with the
105 same spatial coverage and resolution. In particular, considering that there are few public datasets of
106 these three gaseous pollutants with such spatiotemporal coverages focusing on the whole of China,
107 this is highly valuable for the sake of studying their variations, relative proportions, and attribution
108 of emission sources, as well as their diverse and joint effects of different pollutant species on public
109 health.

110

111 **2. Materials and methods**

112 **2.1 Big data**

113 **2.1.1 Ground-based measurements**

114 Hourly measurements of ground-level NO₂, SO₂, and CO concentrations from ~2000 reference-
115 grade ground-based monitoring stations (Figure 1) collected from the China National
116 Environmental Monitoring Centre (CNEMC) network (open-source available at
117 <https://www.cnemc.cn/en/>) were employed in the study. This network includes urban assessing
118 stations, regional assessing stations, background stations, source impact stations, and traffic
119 stations, set up in a reasonable overall layout that covers industrial (~14%), urban (~31%), suburban
120 (~39%), and rural (~16%) areas to improve the spatial representations, continuity, and
121 comparability of observations (HJ 664-2013) (MEE, 2013a). NO₂ is measured by
122 chemiluminescence and differential optical absorption spectroscopy (DOAS), and SO₂ uses
123 ultraviolet fluorescence and DOAS, while CO adopts non-dispersive infrared spectroscopy and gas
124 filter correlation infrared spectroscopy. These measurements have been fully validated and have the
125 same average error of indication of ±2% F.S. for the three gaseous pollutants considered here, with
126 additional quality-control checks such as zero and span noise and zero and span drift (HJ 193-2013
127 and HJ 654-2013) (MEE, 2013b, 2013c). They have also been used as ground truth in almost all air
128 pollutant modelling studies in China (Ma et al., 2022; B. Zhang et al., 2022a). All stations use the
129 same technique to measure each gas routinely and continuously 24 hours a day at about the sea
130 level without time series gaps. However, the reference state (i.e., observational conditions like
131 temperature and pressure) changed from the standard condition (i.e., 273 K and 1013 hPa) to the
132 room condition (i.e., 298 K and 1013 hPa) on 31 August 2018 (MEE, 2018a). We thus first

133 converted observations of the three gaseous pollutants after this date to the uniform standard
134 condition for consistency. Here, daily values for each air pollutant were averaged from at least 30%
135 of valid hourly measurements at each station in each year from 2013 to 2020.

136 *[Please insert Figure 1 here]*

137 **2.1.2 Main predictors**

138 A new daily tropospheric NO₂ dataset at a horizontal resolution of 0.25° × 0.25° in China
139 (<https://doi.org/10.6084/m9.figshare.13126847>) was employed, created by Q. He et al. (2020) using
140 a developed framework integrating OMI/Aura Quality Assurance for Essential Climate Variables
141 (QA4ECV) and Global Ozone Monitoring Experiment–2B (GOME-2B) offline tropospheric NO₂
142 retrievals passing quality controls (i.e., cloud fraction < 0.3, surface albedo < 0.3, and solar zenith
143 angle < 85°). The reconstructed tropospheric NO₂ agreed well (R = 0.75–0.85) with Multi-AXis
144 Differential Optical Absorption Spectroscopy (MAX-DOAS) measurements (H. He et al., 2020).
145 Through this data fusion, the daily spatial coverage of satellite tropospheric NO₂ was significantly
146 improved in China (average = 87%). Areas with a small number of missing values were imputed via
147 a nonparametric machine-learning model by regressing the conversion relationship with Copernicus
148 Atmosphere Monitoring Service (CAMS) tropospheric NO₂ assimilations (0.75° × 0.75°), making
149 sure that the interpolation was consistent with the OMI/Aura overpass time (Inness et al., 2019; Y.
150 Wang et al., 2020). The gap-filled tropospheric NO₂ was reliable compared with measurements (R =
151 0.94–0.98) (Wei et al., 2022b). The above two-step gap-filling procedures allowed us to generate a
152 daily seamless tropospheric NO₂ dataset that removes the effects of clouds from satellite
153 observations.

154 Here, the reconstructed daily seamless tropospheric NO₂, together with CAMS daily ground-level
155 NO₂ assimilations (0.75° × 0.75°) averaged from all 3-hourly data in a day and monthly NO_x
156 anthropogenic emissions (0.1° × 0.1°) (Inness et al., 2019), were used as the main predictors for
157 estimating surface NO₂. Limited by the quality of direct satellite observations, daily model-
158 simulated SO₂ and CO surface mass concentrations, averaged from all available data in a day
159 provided by one-hourly Modern-Era Retrospective Analysis for Research and Applications, version
160 2 (MERRA-2, 0.625° × 0.5°), 3-hourly CAMS (0.75° × 0.75°), and 3-hourly Goddard Earth

161 Observing System Forward-Processing ($0.3125^\circ \times 0.25^\circ$) global reanalyses were used as main
162 predictors to retrieve surface SO₂ and CO, together with CAMS monthly SO₂ and CO
163 anthropogenic emissions.

164

165 2.1.3 Auxiliary factors

166 Meteorological factors have important diverse effects on air pollutants (J. He et al., 2017; R. Li et
167 al., 2019), e.g., the boundary-layer height reflects their vertical distribution and variations (Z. Li et
168 al., 2017; Seo et al., 2017); temperature, humidity, and pressure can affect their photochemical
169 reactions (W. Y. Xu et al., 2011; T. Li et al., 2019; C. Zhang et al., 2019a); and rainfall and wind can
170 also influence their removal, accumulation, and transport (Dickerson et al., 2007; R. Li et al., 2019).
171 Eight daily meteorological variables, provided by the ERA5-Land ($0.1^\circ \times 0.1^\circ$; Muñoz-Sabater et
172 al., 2021) and ERA5 global reanalysis ($0.25^\circ \times 0.25^\circ$; Hersbach et al., 2020), were calculated (i.e.,
173 accumulated for precipitation and evaporation while averaged for the others) from all hourly data in
174 a day, used as auxiliary variables to improve the modelling of gaseous pollutants. Other auxiliary
175 remote-sensing data used to describe land-use cover/change [i.e., Moderate Resolution Imaging
176 Spectroradiometer (MODIS) normalized difference vegetation index (NDVI), $0.05^\circ \times 0.05^\circ$] and
177 population distribution density (i.e., LandScanTM, 1 km) were employed as inputs to the machine-
178 learning model because they are highly related to the type of pollutant emission and amounts of
179 anthropogenic emissions, as well as the surface terrain [i.e., Shuttle Radar Topography Mission
180 (SRTM) digital elevation model (DEM), 90m], which can affect the transmission of air pollutants.
181 Table S1 provides detailed information about all the data used in this study.

182 ~~Major input data employed in the study are hourly routine measurements of the ground-level NO₂,~~
183 ~~SO₂, and CO concentrations of at approximately 2000 reference-grade ground-based monitoring~~
184 ~~stations across China from 2013 to 2020. Due to a change in the reference state implemented on 31~~
185 ~~August 2018 (Mee, 2018), we first converted the concentrations of the three gaseous pollutants to~~
186 ~~the uniform standard condition (i.e., 273 K and 1013 hPa) for consistency. Daily values for each air~~
187 ~~pollutant at each station in each year were then averaged from valid hourly measurements that had~~
188 ~~undergone additional quality control checks.~~

189

2.1.2 Satellite, reanalysis, and model data

Satellite remote sensing data used here include the daily seamless tropospheric NO₂ products (0.25° × 0.25°) generated by first combining OMI/Aura and Global Ozone Monitoring Experiment 2B retrievals (He et al., 2020), and then gap-filling using CAMS tropospheric NO₂ simulations via machine learning (Wei et al., 2022b), and MODIS monthly NDVI (0.05° × 0.05°), LandScanTM annual population (POP, 1 km) (Bright et al., 2000), and the SRTM digital elevation model (DEM, 90 m). ERA5 Land (0.1° × 0.1°) and ERA5 global reanalysis (0.25° × 0.25°) provided hourly meteorological fields (Muñoz-Sabater et al., 2021; Hersbach et al., 2020). The following eight variables from the reanalysis are employed in our study: 2-m temperature (TEM), precipitation (PRE), evaporation (ET), 10-m u- and v- components of wind (WU and WV), boundary layer height (BLH), relative humidity (RH), and surface pressure (SP). Besides, model-simulated SO₂ and CO surface mass concentrations were also included from the MERRA-2 and GEOS-FP global reanalysis every 1 and 3 hours at horizontal resolutions of 0.625° × 0.5° and 0.3125° × 0.25°, respectively. CAMS global reanalysis provided three-hour NO₂ simulations modeled on the earth's surface (every 3 hours, with a horizontal resolution of 0.75° × 0.75°) (Inness et al., 2019). Monthly 0.1° × 0.1° anthropogenic emissions, i.e., NO_x, SO₂, and CO, were collected from CAMS global emission inventories. Here, for these fine temporal resolution variables, all hourly-level simulations in a day were first averaged for each grid to calculate daily means. All variables were aggregated or resampled into a 0.1° × 0.1° resolution for consistency.

2.2 Pollutant gas modelling

Here, the developed Space-Time Extra-Tree (STET) model, integrating spatiotemporal autocorrelations of and differences in air pollutants to the Extremely Randomized Trees (ERT) (Wei et al., 2022a), was extended to estimate surface gaseous pollutants, i.e., NO₂, SO₂, and CO. ERT is an ensemble machine-learning model based on the decision tree, capable of solving the nonparametric multivariable nonlinear regression problem. Ensemble learning can avoid the lack of learning ability of a single learner, greatly improving accuracy. The introduced randomness enhances the model's anti-noise ability and minimizes the sensitivity to outliers and multicollinearity issues. It can handle high latitude, discrete or continuous data without data

219 normalization and is easy to implement and parallel. However, several limitations exist, e.g., it is
 220 difficult to make predictions beyond the range of training data, and there will be an over-fitting
 221 issue on some regression problems with high noise. The training efficiency diminishes with
 222 increasing memory occupation when the number of decision trees is large (Geurts et al., 2006).
 223 Compared with traditional tree-based models (e.g., random forest), ERT has a stronger randomness
 224 which randomly selects a feature subset at each node split and randomly obtains the optimal branch
 225 attributes and thresholds. This helps to create more independent decision trees, further reducing
 226 model variance and improving training accuracy (Geurts et al., 2006). The STET model has been
 227 successfully applied in estimating high-quality surface O₃ in our previous study (Wei et al., 2022a).
 228 It is thus extended here to regress the nonlinear conversion relationships between ground-based
 229 measurements and the main predictors and auxiliary factors for other species of gaseous pollutants.

230 For surface NO₂, the STET model was applied to the main variables of the satellite tropospheric
 231 NO₂ column, modelled surface NO₂ mass, and NO_x emissions, together with ancillary variables of
 232 the previously mentioned meteorological, surface, and population variables (Equation 1). For
 233 surface SO₂ (Equation 2) and CO (Equation 3), modelled surface SO₂ and CO concentrations and
 234 SO₂ and CO emissions were used as main predictors along with the same auxiliary variables as NO₂
 235 to construct the STET models separately.

$$237 \quad NO_{2(ijt)} \sim f_{STET}(SNO_{2(ijt)}, MNO_{2(ijt)}, ENO_{x_{ijm}}, Meteorology_{ijt}, NDVI_{ijm}, DEM_{ijy}, POP_{ijy}, P_s, P_t), \quad (1)$$

$$238 \quad SO_{2(ijt)} \sim f_{STET}(MSO_{2(ijt)}, ESO_{2(ijm)}, Meteorology_{ijt}, NDVI_{ijm}, DEM_{ijy}, POP_{ijy}, P_s, P_t), \quad (2)$$

$$239 \quad CO_{ijt} \sim f_{STET}(MCO_{ijt}, ECO_{ijm}, Meteorology_{ijt}, NDVI_{ijm}, DEM_{ijy}, POP_{ijy}, P_s, P_t), \quad (3)$$

240
 241 where $NO_{2(ijt)}$, $SO_{2(ijt)}$, and CO_{ijt} indicate daily ground-based NO₂, SO₂, and CO measurements at
 242 one grid (i, j) on the t th day of a year; $SNO_{2(ijt)}$ indicates the daily satellite tropospheric NO₂ column
 243 at one grid (i, j) on the t th day of a year; $MNO_{2(ijt)}$, $MSO_{2(ijt)}$, and MCO_{ijt} indicate daily model-
 244 simulated surface NO₂, SO₂, and CO concentrations at one grid (i, j) on the t th day of a year;
 245 $ENO_{x_{ijm}}$, $ESO_{2(ijm)}$, and ECO_{ijm} indicate monthly anthropogenic NO_x, SO₂, and CO emissions at one
 246 grid (i, j) in the m th month of a year; $Meteorology_{ijt}$ represents each meteorological variable at one
 247 grid (i, j) on the t th day of a year; DEM_{ijy} and POP_{ijy} indicate the elevation and population at one

248 grid (i, j) of a year; and P_s and P_t indicate the space and time term (Wei et al., 2022a).

249 ~~Here, two widely used 10-fold out-of-sample and out-of-station cross-validation (CV) methods~~
250 ~~(Wei et al., 2022a; Rodriguez et al., 2010) were employed to assess the data quality. They were~~
251 ~~performed by randomly dividing data samples and ground monitoring stations into independent~~
252 ~~training and testing datasets to evaluate the overall accuracy and prediction reliability, i.e., estimates~~
253 ~~for the samples and predictions for the stations that are excluded from training, respectively. Wei et~~
254 ~~al. (2022a) provides details about how these two methods work.~~

255

256 **3. Results and discussion**

257 **3.1 Model performance**

258 **3.1 Seamless mapping of surface gaseous pollutants**

259 Using the constructed STET model, we generated daily 10 km resolution datasets with complete
260 coverage (spatial coverage = 100%) for three ground-level gaseous pollutants from 2013 to 2020 in
261 China, called ChinaHighNO₂, ChinaHighSO₂, and ChinaHighCO. Monthly and annual maps were
262 generated by directly averaging daily data at each grid. They belong to a series of public high-
263 resolution and high-quality datasets of a variety of ground-level air pollutants for China
264 [ChinaHighAirPollutants (CHAP), available at <https://weijing-rs.github.io/product.html>] developed
265 by our team. Figure 2 shows spatial distributions of the three pollutant gases across China on a
266 typical day (1 January 2018). The spatial patterns of these gaseous pollutants were consistent with
267 those observed on the ground, especially in highly polluted areas, e.g., severe surface NO₂ pollution
268 in the North China Plain (NCP) and high surface SO₂ emissions in Shanxi Province. The unique
269 advantage of our dataset is that it can provide valuable gaseous pollutant information on a daily
270 basis at locations in China where ground measurements are not available. This addresses the major
271 issues of scanning gaps and numerous missing values in satellite remote sensing retrievals at cloudy
272 locations, e.g., the average spatial coverage of the official OMI/Aura daily tropospheric NO₂
273 product is only 42% over the whole of China during the period 2013–2020 (Figure S1). Our dataset
274 provides spatially complete coverage, significantly increasing ~~the daily data utilization~~ satellite
275 observations by 58%. In addition, reanalysis data do not simulate surface masses of gaseous
276 pollutants well, underestimating them compared to our results and ground-based observations in

277 China (Figure S2). This is especially so for SO₂, where high-pollution hot spots are easily
278 misidentified. Validation illustrates that our regressed results for surface NO₂, SO₂, and CO agree
279 better with ground measurements than modelled results (slopes are close to 1, and correlations >
280 0.93), 1.9–6.4 times stronger in slope, 1.3–3.5 times higher in correlation, but 5.9–7.7 times smaller
281 in differences (Figure S3). This shows that our model can take advantage of big data to significantly
282 correct and reconstruct gaseous simulation results via data mining using machine learning.

283 *[Please insert Figure 4₂ here]*

284 Figure 3 shows annual and seasonal maps for each gas pollutant during the period 2013–2020
285 across China. Multi-year mean surface NO₂, SO₂, and CO concentrations were 20.3 ± 4.7 μg/m³,
286 16.2 ± 7.7 μg/m³, and 0.86 ± 0.22 mg/m³, respectively. Pollutant gases varied significantly in space
287 across China, where high surface NO₂ levels were mainly distributed in typical urban
288 agglomerations, e.g., the Beijing-Tianjin-Hebei (BTH) region, the Yangtze River and Pearl River
289 Deltas (YRD and PRD), and scattered large cities with intensive human activities and highly
290 developed transportation systems (e.g., Urumqi, Chengdu, Xi'an, and Wuhan, among others). High
291 surface SO₂ concentrations were mainly observed in northern China (e.g., Shanxi, Hebei, and
292 Shandong Provinces), associated with combustion emissions from anthropogenic sources, and the
293 Yunnan Guizhou Plateau in southwest China, likely associated with emissions from volcanic
294 eruptions. By contrast, except in some areas in central China (e.g., Shanxi and Hebei), surface CO
295 concentrations were overall low.

296 Significant differences in spatial patterns were seen at the seasonal level. Surface NO₂, SO₂, and CO
297 in summer (average = 15.9 ± 4.7 μg/m³, 22.9 ± 13.4 μg/m³, and 1.1 ± 0.3 mg/m³, respectively) were
298 the lowest, thanks to favorable meteorological conditions: e.g., abundant precipitation and high air
299 humidity conducive to flushing and scavenging of different air pollutants (Yoo et al., 2014). Strong
300 sunlight and high temperature also accelerate the photochemical reactions of NO₂ loss (Shah et al.,
301 2020). Pollution levels were highest in winter, with average values increasing by ~1.5–1.9 times
302 those in summer. This difference was much larger in central and eastern China, e.g., 2.3–3.4 times
303 higher in the BTH, due to large amounts of direct NO_x, SO₂, and CO emissions from burning coal
304 for heating in winter in northern China. The spatial patterns of the three gaseous pollutants were

305 similar in spring and autumn.

306 *[Please insert Figure 3 here]*

307 **3.2 Changes in gaseous pollution and exposure risk**

308 **3.1.13.2.1 Short-term epidemic effects on air quality**

309 Many studies have focused on the effects of the COVID-19 epidemic on air quality (WHO, 2020).
310 Most of them were done using ground-based observations (Huang et al., 2020; T. Su et al., 2020),
311 tropospheric gas columns (Field et al., 2021; Levelt et al., 2022), or retrieved surface masses (Ling
312 and Li, 2021; Cooper et al., 2022). The resulting conclusions could be affected by insufficient
313 spatial representation due to the uneven distribution of ground monitors or a large number of
314 missing values in space due to the influence of clouds. The unique advantage of our seamless day-
315 to-day gaseous pollutant dataset can make up for these shortcomings, allowing us to more
316 accurately and quantitatively assess the changes in gaseous pollutants during the epidemic.

317 We first compared the spatial differences in monthly relative differences from February to April
318 between 2020 and 2019 in ~~eastern~~ China (Figure 4). In February, surface NO₂ sharply reduced in
319 China, especially in key urban agglomerations and megacities, showing relative changes of greater
320 than 50%. A significant decrease in surface SO₂ (> 40%) was observed in northern areas where
321 heavy industry is the mainstay in China (e.g., Tianjin, Hebei, and Shandong), while little change
322 was seen in southern China. Surface CO also showed drastic decreases, but the amplitude was
323 smaller than the other two gaseous pollutants. These were attributed to extensive plant closures and
324 traffic controls due to the lockdown, which started at the end of January 2020, significantly
325 reducing anthropogenic NO_x, SO₂, and CO emissions (Ding et al., 2020; Zheng et al., 2021). In
326 March, surface NO₂ was still generally lower than the historical level in most eastern areas,
327 especially in areas where the epidemic was severe, i.e., Wuhan, Hubei Province, and its surrounding
328 areas. The decrease in surface SO₂ largely slowed by more than two times in the NCP and central
329 China, while surface CO almost returned to normal levels in most areas in China. In April, surface
330 NO₂ and SO₂ were comparable to historical concentrations (within $\pm 10\%$), even increasing in some
331 areas of southern and northeastern areas due to rebounding anthropogenic emissions (Ding et al.,
332 2020), especially in Hubei Province, indicating that their surface levels were almost recovered.

333 *[Please insert Figure 4 here]*

334 Most previous studies have focused mainly on changes during the lockdown, with little attention
335 paid to the recovery. We thus compared the time series of daily population-weighted concentrations
336 of the three gaseous pollutants after the Lunar New Year between 2020 and 2019 in China (Figure
337 5). After the beginning of New Year's Eve, surface gaseous pollutants showed a significant decrease
338 in both the normal and epidemic years due to the closure of factories, with decreasing
339 anthropogenic emissions during the Spring Festival holiday. However, gaseous pollutants in the
340 normal year rose rapidly after they fell to their lowest levels due to the return to work after the
341 holidays. By contrast, their levels continued to decrease in 2020 and were lower than historical
342 levels due to the sustained impacts of the strict lockdowns. They hit bottom in the 4th week after the
343 Lunar New Year, then began to increase gradually. Surface NO₂ and SO₂ recovered in the middle of
344 the 11th week (around the 72nd and 75th days) after the Lunar New Year. However, surface CO levels
345 recovered at the end of the 5th week (around the 34th day), more than twice faster than NO₂ and SO₂
346 levels. This is attributed to more CO emissions from increased residents' indoor cooking (Zheng et
347 al., 2018), increased atmospheric oxidation capacity (Huang et al., 2020; Wei et al., 2022a), and a
348 potentially higher sensitivity to temperature rises (Lin et al., 2021).

349 *[Please insert Figure 5 here]*

350 **3.2.2 Temporal variations and policy implications**

351 Figures S4-S6 show annual mean maps of each gaseous pollutant from 2013 to 2020 in China.
352 Surface NO₂, SO₂, and CO changed greatly, peaking in 2013, with average values of 21.3 ± 8.8
353 $\mu\text{g}/\text{m}^3$, $23.1 \pm 13.3 \mu\text{g}/\text{m}^3$, and $1.01 \pm 0.29 \text{ mg}/\text{m}^3$, respectively. They reached their lowest levels in
354 2020, particularly due to the noticeable effects of the COVID-19 epidemic. In general, national
355 ambient NO₂, SO₂, and CO concentrations decreased by approximately 12%, 55%, and 17% from
356 2013 to 2020, respectively. Large seasonal differences were observed in the amplitude of gaseous
357 pollutant (Figure 6), e.g., surface NO₂ decreased the most in winter, especially in the three urban
358 agglomerations ($\downarrow 24$ – 31%), changing the least in autumn (especially in the YRD). Surface SO₂
359 showed much larger decreases in all seasons, especially during the cold seasons ($\downarrow 55$ – 81%), due to
360 the implementation of stricter “ultra-low” emission standards (Q. Zhang et al., 2019; Li et al.,

361 2022a). Surface CO had similar seasonal changes as SO₂ but 1.5–3.3 times smaller in amplitude.

362 [Please insert Figure 6 here]

363 **3.1.2 Long-term trends and policy implications**

364 To better investigate the spatiotemporal variations of ambient gaseous pollution, we calculated
365 linear trends and significance levels using monthly anomalies by removing seasonal cycles. ~~Given~~
366 ~~that monitoring stations were sparse and unevenly distributed in western China, especially in earlier~~
367 ~~years, we will focus on eastern part of the country for the trend analysis.~~ Most of eastern China
368 showed ~~more~~ significant decreasing trends, with average annual rates of 0.23 µg/m³, 2.01 µg/m³,
369 and 0.05 mg/m³ for surface NO₂, SO₂, and CO ($p < 0.001$), respectively (Figure 7), especially in
370 three urban agglomerations (~~trend = -0.51--1.21 µg/m³/yr, $p < 0.001$), as well as in other and~~ large
371 cities (e.g., Wuhan and Chengdu) (~~Figure 8, and Table 3~~). The largest downward trends mainly
372 occurred in northern and central China, especially in the BTH (~~trend = -6.01 and 109 µg/m³/yr, $p <$~~
373 ~~0.001, respectively).~~ Table 3). This is mainly due to the change in fuel for heating from coal to gas
374 widespread across China in winter (S. Wang et al., 2020), greatly reducing ~~the~~ emissions of
375 precursor gases (Koukouli et al., 2018). Increasing trends of surface NO₂ were, however, found in
376 Ningxia and Shanxi Provinces in central China due to increased traffic emissions and new coal-
377 burning power plants in underdeveloped areas without strict regulations on NO_x emissions (van der
378 A et al., 2017; Maji and Sarkar, 2020; C. Li et al., 2022).

379 We then divided the study period into three periods to investigate the impact of major
380 environmental protection policies on air quality implemented in China (Figure 7). During the Clear
381 Air Action Plan (CAAP, 2013–2017), the rates of decrease for surface NO₂, SO₂, and CO
382 accelerated in most populated areas in China, especially urban areas. This was due to dramatic
383 reductions in main pollutant emissions like SO₂ and NO_x (by 59% and 21%, respectively) through
384 the upgrading of key industries, industrial structure adjustments, and coal-fired boiler remediation
385 (Q. Zhang et al., 2019). In addition, the majority of gaseous pollutants had dropped continuously
386 during the Blue Sky Defense War (BSDW, 2018–2020), benefiting from continuous reductions in
387 total air pollutant emissions and the impacts of COVID-19 (Jiang et al., 2021; Zheng et al., 2021).
388 However, areas with trends passing the significance level sharply shrank, especially for surface

389 SO₂.
390 During the 13th Five-Year-Plan (FYP, 2016–2020), the decreasing trends of the three gaseous
391 pollutants across China slowed down compared to those during CAAP. Large decreases in surface
392 NO₂ were mainly found in the BTH region and Henan Province, while slightly increasing trends
393 occurred in southern China. Surface SO₂ significantly decreased in most areas, where a greater
394 downward trend was observed in Shanxi Province, mainly due to the reduction in coal consumption
395 thanks to a strengthened clean-heating policy (Lee et al., 2021). Surface CO also continuously
396 decreased, more rapidly in central China but less rapidly elsewhere. The continuous decline in
397 gaseous pollutants is due to the binding reductions in total emissions of major pollutants like NO_x
398 (↓71%) and SO₂ (↓48%) in China (Wan et al., 2022; X. Wu et al., 2022).

399 *[Please insert Figure 7 here]*

400 3.2.3 Population-risk exposure to gaseous pollution

401 With the daily seamless datasets, we can evaluate the spatial and temporal variations of short-term
402 population-risk exposure to the three gaseous pollutants by calculating the number of days
403 ~~exceeding their respective air quality standard (Level 2 limitation)~~ in a given year ~~to evaluate the~~
404 ~~distribution and variations of short term pollution exposure (Figure 9). The areal extent of regions~~
405 ~~exposed to unacceptably high pollutant gas exceeding the new recommended short-term minimum~~
406 ~~interim target (IT1) and desired air quality guidelines (AQG) level defined by the WHO in 2021~~
407 ~~(WHO, 2021). The area exceeding the recommended~~ levels (i.e., daily NO₂ > ~~80~~120 µg/m³, SO₂ >
408 ~~150~~125 µg/m³, and CO > ~~4~~7 mg/m³) ~~was generally small in eastern China (Figure S7).~~
409 ~~High NO₂-exposure risks were usually small. NO₂ pollution was mainly found in the NCP Beijing~~
410 ~~and Hebei Province~~ and a handful of big cities (e.g., ~~Xi'an~~Jinan, Wuhan, ~~Shanghai, and~~ Guangzhou,
411 ~~and Shanghai), changing little over time. Surface), while high SO₂ pollution was exposure risks~~
412 ~~were~~ mainly observed in ~~in central China (e.g., Hebei, Shandong, and Shanxi), with the areal extent~~
413 ~~of Shaanxi Provinces. The risk of high CO pollution was small, only found in some scattered areas~~
414 ~~in the NCP. In general, both the area and the possibility of occurrence exposure to high pollution~~
415 ~~has gradually decreased over time, almost disappearing since 2018.~~
416 By contrast, most areas of eastern China had a surface NO₂ exposure exceeding the AQG level

417 (Figure 8), especially in the north and economically developed areas in the south (proportion >
418 80%). Both the extent and intensity are decreasing over time, but it is still a problem, suggesting
419 that stronger NO_x controls are needed in the future. Most of the main air pollution transmission belt
420 in China (i.e., the “2 + 26” cities, Figure 1) had surface SO₂ levels exceeding the AQG level at the
421 beginning of the study period. Thanks to strict control measures, these polluted regions gradually
422 decreasing over time until almost disappearing by 2020. The same was seen for surface CO
423 pollution, being worst in the BTH region and its surrounding areas before 2018, then areas sharply
424 decreased after 2015, almost disappearing by 2020. Surface NO₂ pollution was mainly observed in
425 developed urban areas (e.g., Beijing, Tianjin, Shijiazhuang, and Wuhan), with 15 in 2020.
426 Controlling CO was much more successful in China, with less than 10% of the days in the BTH
427 exceeding the acceptable standard in the early part of the study period, then decreasing to below 5%
428 afterward. Most areas have reached the CO AQG level since 2018.

429 *[Please insert Figure 9 here]*

430 Figure 9 shows the percentage of days with pollution levels exceeding national WHO air quality
431 standards are seen (Figure 10). For example, the in three key regions. BTH region was the only
432 region experiencing a high NO₂ and SO₂ exposure risk, risks (i.e., daily mean > IT1), dropping to
433 zero since 2017 and 2016, while YRD and PRD had no high risks of exposure to the three gaseous
434 pollutants (Figure 9a-b). There was also no regional high CO-pollution risk (Figure 9c). However,
435 although declining continuously, regional surface NO₂ levels failed to meet the short-term AQG
436 level in 2020, with 61–73% of the days exceeding the AQG level. More efforts toward mitigating
437 NO₂ levels in these key regions are thus needed. Continual decreases in the number of days above
438 the AQG level were also observed in surface SO₂, reducing to near zero in 2014, 2016, and 2018 in
439 the PRD, YRD, and BTH, respectively. Less than 3% of the days in the BTH and YRD had surface
440 CO levels exceeding the AQG level. Surface CO levels were always below the AQG level in the
441 PRD.

442 *[Please insert Figure 9 here]*

443 **3.3 Data quality assessment**

444 Here, the widely used out-of-sample 10-fold cross-validation (10-CV) method was adopted to
445 evaluate the overall estimation accuracy of gaseous pollutants (Rodriguez et al., 2010; Wei et al.,
446 2022a). An additional out-of-station 10-CV approach was used to validate the prediction accuracy
447 of gaseous pollutants, performed based on measurements from ground monitoring stations. These
448 measurements were randomly divided into ten subsets, of which gradually lessened data samples
449 from nine subsets were used for model training and the remaining subset for model validation. This
450 was done 10 times, in turn, to ensure that data from all stations were tested. This procedure
451 generates independent training samples and test samples made in different locations, used to
452 indicate the spatial prediction ability of the model in areas where ground-based measurements are
453 unavailable (S. Wu et al., 2021; Wei et al., 2022a).

454

455 **3.3.1 Estimate and prediction accuracy**

456 Figure 10 shows the CV results of all daily estimates and predictions for ground-level NO₂, SO₂,
457 and CO concentrations from 2013 to 2020 in China (sample size: $N \approx 3.6$ million). Surface NO₂
458 and SO₂ concentrations mainly fell in the range of 200 to 500 $\mu\text{g}/\text{m}^3$. Daily estimates were highly
459 correlated to observations, with the same coefficients of determination ($R^2 = 0.84$) and slopes close
460 to 1 (0.86 and 0.84, respectively). Average root-mean-square error (RMSE) [mean absolute error
461 (MAE)] values of surface NO₂ and SO₂ estimates were 7.99 (5.34) and 10.07 (4.68) $\mu\text{g}/\text{m}^3$, and
462 normalized RMSE (NRMSE) values were 0.25 and 0.51, respectively. Most daily CO observations
463 were less than 10 mg/m^3 , agreeing well with our daily estimates ($R^2 = 0.80$, slope = 0.79), and the
464 average RMSE (MAE) and NRMSE values were 0.29 (0.16) mg/m^3 and 0.3. Compared to
465 estimation accuracies (Figure 10a-c), prediction accuracies slightly decreased, which is acceptable
466 considering the weak signals of trace gases. Daily surface SO₂, NO₂, and CO predictions (Figure
467 10d-f) agree well with ground measurements, with spatial R^2 values of 0.70, 0.68, and 0.61,
468 respectively. Their respective RMSE (MAE) values were 14.28 (8.1) $\mu\text{g}/\text{m}^3$, 11.57 (7.06) $\mu\text{g}/\text{m}^3$,
469 and 0.42 (0.24) mg/m^3 , and NRMSE values were 0.35, 0.71, and 0.42, respectively, representing the
470 accuracy for areas without ground monitoring stations.

471

[Please insert Figure 10 here]

472 The performance of our air pollution modelling was also evaluated on an annual basis, showing that
473 our model works well in estimating and predicting the concentrations of different surface gaseous
474 pollutants in different years (Table 1). The model performance has continuously improved over
475 time, as indicated by increasing correlations and decreasing uncertainties. This is because of the
476 increasing density of ground stations (especially in the suburban areas of cities) and updated quality
477 control of measurements, e.g., improving the sampling flow calibration of monitoring instruments,
478 flow calibration of dynamic calibrators, and revision of precision/accuracy review and data validity
479 judgment (HJ 818-2018) (MEE, 2018b). This has led to an increase in the number of data samples
480 (e.g., from 169 thousand in 2013 to more than 522 thousand in 2020) and improvement in their
481 quality.

482 *[Please insert Table 1 here]*

483 Figure 11 shows the spatial validation of estimated daily pollutant gases across China. In general,
484 our model works well at the site scale, with average CV-R² values of 0.77, 0.72, and 0.72, and
485 NRMSE values of 0.25, 0.43, and 0.26 for surface NO₂, SO₂, and CO, respectively. In addition,
486 approximately 93%, 80%, and 84% of the stations had at least moderate agreements (CV-R² > 0.6)
487 between our estimates and ground measurements. Except for some scattered sites, the estimation
488 uncertainties were generally less than 0.3, 0.5, and 0.3 in more than 80%, 77%, and 76% of the
489 stations for the above three gaseous pollutant species, respectively.

490 *[Please insert Figure 11 here]*

491 Figure 12 shows the temporal validation of ground-level gaseous pollutants as a function of ground
492 measurements in China. On the monthly scale (Figure 12a-c), we collected a total of ~119,000
493 matched samples of the three gaseous pollutants. Accuracies significantly improved, with increasing
494 R² (decreasing RMSE) values of 0.93 (4.41 μg/m³), 0.97 (4.03 μg/m³), and 0.94 (0.13 mg/m³) for
495 surface NO₂, SO₂, and CO, respectively. On the annual scale (Figure 12d-f), more than ~10,000
496 matched samples were collected, showing better agreement with observations (e.g., R² = 0.94, 0.98,
497 and 0.97) and lower uncertainties (e.g., RMSE = 3.06 μg/m³, 2.46 μg/m³, and 0.07 mg/m³) for the
498 above three gaseous pollutants, respectively.

499

[Please insert Figure 12 here]

500

3.3.2 Comparison with previous studies

501

We compared our results with those from previous studies on the estimation of the three gaseous

502

pollutants using different developed models focusing on the whole of China. Here, only those

503

studies applying the same out-of-sample cross-validation approach against ground-based

504

measurements collected from the same CNEMC network were selected (Table 2). The statistics

505

shown in the table come from the publications themselves because their generated datasets are not

506

publicly available. We have applied the same validation method and ground measurements as those

507

used in the previous studies. Most generated surface NO₂ datasets had ~~low spatial resolutions~~

508

~~($0.125^{\circ} \times 0.25^{\circ}$)~~ with numerous missing values in space limited by direct OMI/Aura satellite

509

observations at spatial resolutions from $0.125^{\circ} \times 0.125^{\circ}$ to $0.25^{\circ} \times 0.25^{\circ}$ (Zhan et al., 2018; ~~Dou et~~

510

~~al., 2021; Z.-Y. Chen et al., 2019; H. Xu et al., 2019; Chi et al., 2021; Dou et al., 2021).~~ Some

511

studies improved the spatial ~~resolutions~~resolution by introducing NO₂ data from the recently

512

launched Sentinel-5 TROPOMI satellite, but ~~and data are~~ only provide dataset after available from

513

October 2018 onward (~~Chi et al., 2022;~~ Liu, 2021; Y. Wang et al., 2021; Chi et al., 2022; Wei et al.,

514

2022b). Surface SO₂ estimated from ~~an~~ SO₂ emission inventory and surface CO from ~~the~~

515

Measurement of Pollution in the Troposphere (MOPITT) and TROPOMI retrievals have a much

516

lower data quality, with smaller R² values by 12–57% and larger RMSE values by 41–47% against

517

ground measurements compared to ours (~~Li et al., 2020; D. Liu et al., 2019; R. Li et al., 2020; Y.~~

518

~~Wang et al., 2021)~~ have a much lower data quality (~~Li et al., 2020; Li et al., 2017b; Wang et al.,~~

519

~~2021).~~ Overall, our gaseous pollutant datasets are superior to those from previous studies in terms

520

of overall accuracy, spatial coverage, and length of data records.

521

[Please insert Table 2 here]

522

3.3.3.4 Successful applications

523

Our surface gaseous pollutant datasets have been freely available to the public online since March

524

2021 (NO₂: <https://doi.org/10.5281/zenodo.4641542>, SO₂: <https://doi.org/10.5281/zenodo.4641538>,

525

and CO: <https://doi.org/10.5281/zenodo.4641530>). A large number of studies have used the three

526

gaseous pollutant datasets generated in this study to study their single or joint impacts on

527 environmental health from both long-term and short-term perspectives, benefiting from the unique
528 daily spatially seamless coverage. For example, a nearly linear relationship between long-term
529 ambient NO₂ and adult mortality in China was observed (Y. Zhang et al., 2022). Y. Wang et al.
530 (2023) reported that ambient NO₂ hindered the survival of middle-aged and elderly people. Long-
531 term SO₂ and CO exposure can increase the incidence rate of visual impairment in children in China
532 (L. Chen et al., 2022a), and short-term exposure to ambient CO can significantly increase the
533 probability of hospitalization for stroke sequelae (R. Wang et al., 2022). Regional and national
534 cohort studies have shown that exposure, especially short-term exposure, to multiple ambient
535 gaseous (NO₂, SO₂, and CO) and particulate pollutants have negative effects of varying degrees on
536 a variety of diseases, like cause-specific cardiovascular disease (R. Xu et al., 2022a,b), ischemic and
537 hemorrhagic stroke (Cai et al., 2022; He et al., 2022; H. Wu et al., 2022b; R. Xu et al., 2022c),
538 asthma mortality (W. Liu et al., 2022), dementia mortality (T. Liu et al., 2022), metabolic syndrome
539 (S. Han et al., 2022), blood pressure (Song et al., 2022; H. Wu et al., 2022a), renal function (S. Li et
540 al., 2022), neurodevelopmental delay (X. Su et al., 2022), serum liver enzymes (Y. Li et al., 2022),
541 overweight and obesity (L. Chen et al., 2022b), insomnia (J. Xu et al., 2021), and sleep quality (L.
542 Wang et al., 2022). These studies attest well to the value of the CHAP dataset regarding current and
543 future public health issues, among others. and have now been successfully employed for various
544 application studies in environment and health. Strong associations and negative effects between
545 ambient gaseous pollution (e.g., NO₂, SO₂, and CO) and a variety of diseases has been
546 demonstrated for people of all ages through multi-regional and national cohort studies in China.
547 These diseases include general mortality (Zhang et al., 2022), cause-specific cardiovascular disease
548 (Xu et al., 2022a), ischemic and hemorrhagic stroke (Xu et al., 2022b; Wu et al., 2022b; Cai et al.,
549 2022; He et al., 2022), dementia mortality (Liu et al., 2022), blood pressure (Song et al., 2022; Wu
550 et al., 2022a), renal function (Li et al., 2022a), neurodevelopmental delay (Su et al., 2022), serum
551 liver enzymes (Li et al., 2022b), overweight and obesity (Chen et al., 2022b), insomnia (Xu et al.,
552 2021), subjective sleep quality (Wang et al., 2022), and visual impairment (Chen et al., 2022a).
553 These studies attest well to the value of the CHAP dataset with some unique merits for the sake of
554 public health, among others, now and in the future.

555

556 4. Summary and conclusions

557 Exposure to gaseous pollution is detrimental to human health, a major public concern in heavily
558 polluted regions like China, where ground-based observations are not as rich as in major developed
559 countries. Moreover, pollutants travel long distances, affecting large downstream regions. To
560 remedy such limitations, this study applied the machine-learning model called Space-Time Extra-
561 Tree to estimate ambient gaseous pollutants across China, with extensive input variables measured
562 by monitors and satellites, and models. Daily 10 km resolution (approximately $0.1^\circ \times 0.1^\circ$) seamless
563 (spatial coverage = 100%) datasets for ground-level NO₂, SO₂, and CO concentrations in China
564 from 2013 to 2020 were generated. These datasets were cross-evaluated in terms of overall
565 accuracy and predictive ability at different spatiotemporal levels. National daily estimates
566 (predictions) of surface NO₂, SO₂, and CO were highly consistent with ground measurements, with
567 average out-of-sample (out-of-station) CV-R² values of 0.84 (0.68), 0.84 (0.7), and 0.8 (0.61), and
568 RMSEs of 7.99 (11.57) $\mu\text{g}/\text{m}^3$, 10.7 (14.28) $\mu\text{g}/\text{m}^3$, and 0.29 (0.42) mg/m^3 , respectively.

569 Ambient pollutant gases varied significantly in space and time, with high levels mainly found in the
570 North China Plain, especially in winter, due to more anthropogenic emissions, such as coal burning
571 for heating. All gaseous pollutants sharply declined in China during the COVID-19 outbreak, while
572 large differences were observed during their recovery times. For example, surface CO was the first
573 to return to its historical level within the fifth week after the Lunar New Year in 2020, about twice
574 faster as surface NO₂ and SO₂ levels. This is attributed to more home cooking and enhanced
575 atmospheric oxidation. Temporally, surface NO₂, SO₂, and CO levels in China gradually decreased
576 from peaks in 2013 (average = $21.3 \pm 8.8 \mu\text{g}/\text{m}^3$, $23.1 \pm 13.3 \mu\text{g}/\text{m}^3$, and $1.01 \pm 0.29 \text{mg}/\text{m}^3$,
577 respectively), with annual rates of decrease of $0.23 \mu\text{g}/\text{m}^3$, $2.01 \mu\text{g}/\text{m}^3$, and $0.05 \text{mg}/\text{m}^3$,
578 respectively ($p < 0.001$), until 2020. Improvements in air quality have been made in the last eight
579 years, thanks to the implementation of a series of environmental protection policies, greatly
580 reducing pollutant emissions. In addition, both the areal extents of regions experiencing gaseous
581 pollution and the probability of gaseous pollution occurring have gradually decreased over time,
582 especially for surface CO and SO₂, which have almost reached the short-term air quality guidelines
583 level recommended by the WHO in most areas in China in 2020. This high-quality daily seamless
584 dataset of gaseous pollutants will benefit future environmental and health-related studies focused on

585 China, especially studies investigating short-term air pollution exposure.

586 Although a lot of new and/or useful data and analyses are presented in this study, they still suffer
587 from some limitations. For example, input variables related to the emission inventory, modeled
588 simulations, and assimilations still have considerable uncertainties. More influential factors
589 stemming from regional economic and development differences need to be considered in more
590 powerful artificial intelligence models to improve the prediction accuracy of air pollutants. The
591 spatiotemporal resolutions of gaseous pollutants will be further improved by integrating information
592 from polar-orbiting and geostationary satellites to investigate diurnal variations. In a future study,
593 we will also reconstruct data records over the last two decades and investigate their long-term
594 spatiotemporal variations, filling the gap of missing observations. This will help us understand their
595 formation mechanisms and impacts on fine particulate matter and ozone pollution in China.

596

597 **Data availability**

598 CNEMC measurements of gaseous pollutants are available at <http://www.cnemc.cn>. The
599 reconstructed OMI/Aura tropospheric NO₂ product is available at
600 <https://doi.org/10.6084/m9.figshare.13126847>. MODIS series products and the MERRA-2
601 reanalysis are available at <https://search.earthdata.nasa.gov/>. The SRTM DEM is available at
602 <https://www2.jpl.nasa.gov/srtm/>, and LandScanTM population information is available at
603 <https://landscan.ornl.gov/>. The ERA5 reanalysis is available at <https://cds.climate.copernicus.eu/>,
604 GEOS CF data are available at <https://portal.nccs.nasa.gov/datashare/gmao/>, and the CAMS
605 reanalysis and emission inventory are available at <https://ads.atmosphere.copernicus.eu/>.

606

607 **CHAP dataset availability**

608 The ChinaHighAirPollutants (CHAP) dataset is open access and freely available at <https://weijing->
609 <rs.github.io/product.html>. The ChinaHighNO₂ dataset is available at
610 <https://doi.org/10.5281/zenodo.4641542>, the ChinaHighSO₂ dataset is available at
611 <https://doi.org/10.5281/zenodo.4641538>, and the ChinaHighCO dataset is available at
612 <https://doi.org/10.5281/zenodo.4641530>.

613

614 **Competing interests**

615 The authors declare that they have no conflict of interest.

616

617 **Acknowledgments**

618 JW, ZL, and JW were supported by NASA grants 80NSSC21K1980 and 80NSSC19K0950. PG was

619 supported by NASA's Research Opportunities in Space and Earth Science (ROSES-2020), Program

620 Element A.38: Health and Air Quality Applied Sciences Team.

621

622 **References**

- 623 Anenberg, S. C., Mohegh, A., Goldberg, D. L., Kerr, G. H., Brauer, M., Burkart, K., Hystad, P.,
624 Larkin, A., Wozniak, S., and Lamsal, L.: Long-term trends in urban NO₂ concentrations and
625 associated paediatric asthma incidence: estimates from global datasets, *The Lancet Planetary*
626 *Health*, 6, e49-e58, [https://doi.org/10.1016/S2542-5196\(21\)00255-2](https://doi.org/10.1016/S2542-5196(21)00255-2), 2022.
- 627 Cai, M., Zhang, S., Lin, X., Qian, Z., McMillin, S. E., Yang, Y., Zhang, Z., Pan, J., and Lin, H.:
628 Association of ambient particulate matter pollution of different sizes with in-hospital case
629 fatality among stroke patients in China, *Neurology*, 98(24), e2474-e2486,
630 <https://doi.org/10.1212/WNL.0000000000200546>, 2022.
- 631 Chen, G., Wang, Y., Li, S., Cao, W., Ren, H., Knibbs, L. D., Abramson, M. J., and Guo, Y.:
632 Spatiotemporal patterns of PM₁₀ concentrations over China during 2005–2016: a satellite-
633 based estimation using the random forests approach, *Environmental Pollution*, 242, 605–613,
634 <https://doi.org/10.1016/j.envpol.2018.07.012>, 2018.
- 635 Chen, L., Wei, J., Ma, T., Gao, D., Wang, X., Wen, B., Chen, M., Li, Y., Jiang, J., Wu, L., Li, W.,
636 Liu, X., Song, Y., Guo, X., Dong, Y., and Ma, J.: Ambient gaseous pollutant exposure and
637 incidence of visual impairment among children and adolescents: findings from a longitudinal,
638 two-center cohort study in China, *Environmental Science and Pollution Research*, 29(48),
639 73,262–73,270, <https://doi.org/10.1007/s11356-022-20025-3>, 2022a.
- 640 Chen, L., Gao, D., Ma, T., Chen, M., Li, Y., Ma, Y., Wen, B., Jiang, J., Wang, X., Zhang, J., Chen,
641 S., Wu, L., Li, W., Liu, X., Guo, X., Huang, S., Wei, J., Song, Y., Ma, J., and Dong, Y.: Could
642 greenness modify the effects of physical activity and air pollutants on overweight and obesity
643 among children and adolescents?, *Science of The Total Environment*, 832, 155117,
644 <https://doi.org/10.1016/j.scitotenv.2022.155117>, 2022b.
- 645 Chen, Z.-Y., Zhang, R., Zhang, T.-H., Ou, C.-Q., and Guo, Y.: A kriging-calibrated machine learning
646 method for estimating daily ground-level NO₂ in mainland China, *Science of The Total*
647 *Environment*, 690, 556–564, <https://doi.org/10.1016/j.scitotenv.2019.06.349>, 2019.
- 648 Chi, Y., Fan, M., Zhao, C., Sun, L., Yang, Y., Yang, X., and Tao, J.: Ground-level NO₂ concentration
649 estimation based on OMI tropospheric NO₂ and its spatiotemporal characteristics in typical
650 regions of China, *Atmospheric Research*, 264, 105821,
651 <https://doi.org/10.1016/j.atmosres.2021.105821>, 2021.
- 652 Chi, Y., Fan, M., Zhao, C., Yang, Y., Fan, H., Yang, X., Yang, J., and Tao, J.: Machine learning-
653 based estimation of ground-level NO₂ concentrations over China, *Science of The Total*
654 *Environment*, 807, 150721, <https://doi.org/10.1016/j.scitotenv.2021.150721>, 2022.
- 655 [Cooper, M. J., Martin, R. V., Hammer, M. S., Levelt, P. F., Veefkind, P., Lamsal, L. N., Krotkov, N.](https://doi.org/10.1038/s41586-021-04229-0)
656 [A., Brook, J. R., and McLinden, C. A.: Global fine-scale changes in ambient NO₂ during](https://doi.org/10.1038/s41586-021-04229-0)
657 [COVID-19 lockdowns, *Nature*, 601, 380–387, <https://doi.org/10.1038/s41586-021-04229-0>,](https://doi.org/10.1038/s41586-021-04229-0)
658 [2022.](https://doi.org/10.1038/s41586-021-04229-0)
- 659 [Dickerson, R. R., Li, C., Li, Z., Marufu, L. T., Stehr, J. W., McClure, B., Krotkov, N., Chen, H.,](https://doi.org/10.1029/2007JD008999)
660 [Wang, P., Xia, X., Ban, X., Gong, F., Yuan, J., and Yang, J.: Aircraft observations of dust and](https://doi.org/10.1029/2007JD008999)
661 [pollutants over northeast China: insight into the meteorological mechanisms of transport, 112,](https://doi.org/10.1029/2007JD008999)
662 <https://doi.org/10.1029/2007JD008999>, 2007.
- 663 Ding, J., van der A, R. J., Eskes, H. J., Mijling, B., Stavrou, T., van Geffen, J. H. G. M., and
664 Veefkind, J. P.: NO_x emissions reduction and rebound in China due to the COVID-19 crisis,
665 47, e2020GL089912, <https://doi.org/10.1029/2020GL089912>, 2020.

666 Dou, X., Liao, C., Wang, H., Huang, Y., Tu, Y., Huang, X., Peng, Y., Zhu, B., Tan, J., Deng, Z., Wu,
667 N., Sun, T., Ke, P., and Liu, Z.: Estimates of daily ground-level NO₂ concentrations in China
668 based on random forest model integrated k-means, *Advances in Applied Energy*, 2, 100017,
669 <https://doi.org/10.1016/j.adapen.2021.100017>, 2021.

670 Fang, X., Zou, B., Liu, X., Sternberg, T., and Zhai, L.: Satellite-based ground PM_{2.5} estimation
671 using timely structure adaptive modeling, *Remote Sensing of Environment*, 186, 152–163,
672 <https://doi.org/10.1016/j.rse.2016.08.027>, 2016.

673 [Field, R. D., Hickman, J. E., Geogdzhayev, I. V., Tsigaridis, K., and Bauer, S. E.: Changes in
674 satellite retrievals of atmospheric composition over eastern China during the 2020 COVID-19
675 lockdowns, *Atmos. Chem. Phys.*, 21, 18,333–18,350, \[https://doi.org/10.5194/acp-21-18333-
676 2021\]\(https://doi.org/10.5194/acp-21-18333-2021\), 2021.](#)

677 [Geurts, P., Ernst, D., and Wehenkel, L.: Extremely randomized trees, 36, 3-42,
678 <https://doi.org/10.1007/s10994-006-6226-1>, 2006.](#)

679 [Han, S., Zhang, F., Yu, H., Wei, J., Xue, L., Duan, Z., and Niu, Z.: Systemic inflammation
680 accelerates the adverse effects of air pollution on metabolic syndrome: findings from the China
681 Health and Retirement Longitudinal Study \(CHARLS\), *Environmental Research*, 215, 114340,
682 <https://doi.org/10.1016/j.envres.2022.114340>, 2022.](#)

683 Han, W., He, T. L., Tang, Z., Wang, M., Jones, D., and Jiang, Z.: A comparative analysis for a deep
684 learning model (hyDL-CO v1.0) and Kalman filter to predict CO concentrations in China,
685 *Geosci. Model Dev.*, 15, 4225–4237, <https://doi.org/10.5194/gmd-15-4225-2022>, 2022.

686 He, F., Wei, J., Dong, Y., Liu, C., Zhao, K., Peng, W., Lu, Z., Zhang, B., Xue, F., Guo, X., and Jia,
687 X.: Associations of ambient temperature with mortality for ischemic and hemorrhagic stroke
688 and the modification effects of greenness in Shandong Province, China, *Science of The Total
689 Environment*, 158046, <https://doi.org/10.1016/j.scitotenv.2022.158046>, 2022.

690 [He, J., Gong, S., Yu, Y., Yu, L., Wu, L., Mao, H., Song, C., Zhao, S., Liu, H., Li, X., and Li, R.: Air
691 pollution characteristics and their relation to meteorological conditions during 2014–2015 in
692 major Chinese cities, *Environmental Pollution*, 223, 484–496,
693 <https://doi.org/10.1016/j.envpol.2017.01.050>, 2017.](#)

694 [He, L., Wei, J., Wang, Y., Shang, Q., Liu, J., Yin, Y., Frankenberg, C., Jiang, J., Li, Z., and Yung, Y.:
695 Marked impacts of pollution mitigation on crop yields in China. *Earth's Future*, 10,
696 <https://doi.org/10.1029/2022EF002936>, 2022.](#)

697 He, Q., Qin, K., Cohen, J. B., Loyola, D., Li, D., Shi, J., and Xue, Y.: Spatially and temporally
698 coherent reconstruction of tropospheric NO₂ over China combining OMI and GOME-2B
699 measurements, *Environmental Research Letters*, 15, 125011, [https://doi.org/10.1088/1748-
700 9326/abc7df](https://doi.org/10.1088/1748-9326/abc7df), 2020.

701 Hersbach, H., Bell, B., Berrisford, P., Hirahara, S., Horányi, A., Muñoz-Sabater, J., Nicolas, J.,
702 Peubey, C., Radu, R., Schepers, D., Simmons, A., Soci, C., Abdalla, S., Abellan, X., Balsamo,
703 G., Bechtold, P., Biavati, G., Bidlot, J., Bonavita, M., De Chiara, G., Dahlgren, P., Dee, D.,
704 Diamantakis, M., Dragani, R., Flemming, J., Forbes, R., Fuentes, M., Geer, A., Haimberger, L.,
705 Healy, S., Hogan, R. J., Hólm, E., Janisková, M., Keeley, S., Laloyaux, P., Lopez, P., Lupu, C.,
706 Radnoti, G., de Rosnay, P., Rozum, I., Vamborg, F., Villaume, S., and Thépaut, J.-N.: The
707 ERA5 global reanalysis, 146, 1999–2049, <https://doi.org/10.1002/qj.3803>, 2020.

708 [Huang, X., Ding, A., Gao, J., Zheng, B., Zhou, D., Qi, X., Tang, R., Wang, J., Ren, C., Nie, W., Chi,
709 X., Xu, Z., Chen, L., Li, Y., Che, F., Pang, N., Wang, H., Tong, D., Qin, W., Cheng, W., Liu,](#)

- 710 [W., Fu, Q., Liu, B., Chai, F., Davis, S. J., Zhang, Q., and He, K.: Enhanced secondary pollution](#)
711 [offset reduction of primary emissions during COVID-19 lockdown in China, National Science](#)
712 [Review, 8, <https://doi.org/10.1093/nsr/nwaa137>, 2020.](#)
- 713 Inness, A., Ades, M., Agustí-Panareda, A., Barré, J., Benedictow, A., Blechschmidt, A. M.,
714 Dominguez, J. J., Engelen, R., Eskes, H., Flemming, J., Huijnen, V., Jones, L., Kipling, Z.,
715 Massart, S., Parrington, M., Peuch, V. H., Razinger, M., Remy, S., Schulz, M., and Suttie, M.:
716 The CAMS reanalysis of atmospheric composition, *Atmospheric Chemistry and Physics*, 19,
717 3515–3556, <https://doi.org/10.5194/acp-19-3515-2019>, 2019.
- 718 [Jiang, X., Li, G., and Fu, W.: Government environmental governance, structural adjustment and air](#)
719 [quality: a quasi-natural experiment based on the Three-year Action Plan to Win the Blue Sky](#)
720 [Defense War, Journal of Environmental Management, 277, 111470,](#)
721 <https://doi.org/10.1016/j.jenvman.2020.111470>, 2021.
- 722 Kan, H., Chen, R., and Tong, S.: Ambient air pollution, climate change, and population health in
723 China, *Environment International*, 42, 10–19, <https://doi.org/10.1016/j.envint.2011.03.003>,
724 2012.
- 725 Kinney, P. L.: Climate change, air quality, and human health, *American Journal of Preventive*
726 *Medicine*, 35, 459–467, <https://doi.org/10.1016/j.amepre.2008.08.025>, 2008.
- 727 Koukouli, M. E., Theys, N., Ding, J., Zyrichidou, I., Mijling, B., Balis, D., and van der A, R. J.:
728 Updated SO₂ emission estimates over China using OMI/Aura observations, *Atmospheric*
729 *Measurement Techniques*, 11, 1817–1832, <https://doi.org/10.5194/amt-11-1817-2018>, 2018.
- 730 [Lee, E. J., Kim, M. J., and Lee, J.-S.: Policy implications of the clean heating transition: a case](#)
731 [study of Shanxi, Energies, 14, 8431, <https://doi.org/10.3390/en14248431>, 2021.](#)
- 732 [Levelt, P. F., Stein Zweers, D. C., Aben, I., Bauwens, M., Borsdorff, T., De Smedt, I., Eskes, H. J.,](#)
733 [Lerot, C., Loyola, D. G., Romahn, F., Stavrou, T., Theys, N., Van Roozendaal, M., Veeffkind,](#)
734 [J. P., and Verhoelst, T.: Air quality impacts of COVID-19 lockdown measures detected from](#)
735 [space using high spatial resolution observations of multiple trace gases from Sentinel-](#)
736 [5P/TROPOMI, Atmospheric Chemistry and Physics, 22, 10319–10351,](#)
737 <https://doi.org/10.5194/acp-22-10319-2022>, 2022.
- 738 [Li, C., Hammer, M. S., Zheng, B., and Cohen, R. C.: Accelerated reduction of air pollutants in](#)
739 [China, 2017–2020, Science of The Total Environment, 803, 150011,](#)
740 <https://doi.org/10.1016/j.scitotenv.2021.150011>, 2022.
- 741 [Li, R., Wang, Z., Cui, L., Fu, H., Zhang, L., Kong, L., Chen, W., and Chen, J.: Air pollution](#)
742 [characteristics in China during 2015–2016: spatiotemporal variations and key meteorological](#)
743 [factors, Science of The Total Environment, 648, 902–915,](#)
744 <https://doi.org/10.1016/j.scitotenv.2018.08.181>, 2019.
- 745 Li, R., Cui, L., Liang, J., Zhao, Y., Zhang, Z., and Fu, H.: Estimating historical SO₂ level across the
746 whole China during 1973–2014 using random forest model, *Chemosphere*, 247, 125839,
747 <https://doi.org/10.1016/j.chemosphere.2020.125839>, 2020.
- 748 Li, S., Meng, Q., Laba, C., Guan, H., Wang, Z., Pan, Y., Wei, J., Xu, H., Zeng, C., Wang, X., Jiang,
749 M., Lu, R., Guo, B., and Zhao, X.: Associations between long-term exposure to ambient air
750 pollution and renal function in Southwest China: The China Multi-Ethnic Cohort (CMEC)
751 study, *Ecotoxicology and Environmental Safety*, 242, 113851,
752 <https://doi.org/10.1016/j.ecoenv.2022.113851>, 2022.
- 753 Li, T., Shen, H., Yuan, Q., Zhang, X., and Zhang, L.: Estimating ground-level PM_{2.5} by fusing

- 754 satellite and station observations: a geo-intelligent deep learning approach, 44, 11,985–
755 911,993, <https://doi.org/10.1002/2017GL075710>, 2017.
- 756 Li, Y., Yuan, X., Wei, J., Sun, Y., Ni, W., Zhang, H., Zhang, Y., Wang, R., Xu, R., Liu, T., Yang, C.,
757 Chen, G., Xu, J., and Liu, Y.: Long-term exposure to ambient air pollution and serum liver
758 enzymes in older adults: a population-based longitudinal study, *Annals of Epidemiology*, 74,
759 1–7, <https://doi.org/10.1016/j.annepidem.2022.05.011>, 2022.
- 760 Li, Z., Guo, J., Ding, A., Liao, H., Liu, J., Sun, Y., Wang, T., Xue, H., Zhang, H., and Zhu, B.:
761 Aerosol and boundary-layer interactions and impact on air quality, *National Science Review*, 4,
762 810–833, <https://doi.org/10.1093/nsr/nwx117>, 2017.
- 763 [Lin, J., Lin, C., Tao, M., Ma, J., Fan, L., Xu, R.-A., and Fang, C.: Spatial disparity of
764 meteorological impacts on carbon monoxide pollution in China during the COVID-19
765 lockdown period, *ACS Earth and Space Chemistry*, 5, 2900–2909,
766 <https://doi.org/10.1021/acsearthspacechem.1c00251>, 2021.](#)
- 767 [Ling, C. and Li, Y.: Substantial changes of gaseous pollutants and health effects during the COVID-
768 19 lockdown period across China, *GeoHealth*, 5, e2021GH000408,
769 <https://doi.org/10.1029/2021GH000408>, 2021.](#)
- 770 Liu, J.: Mapping high resolution national daily NO₂ exposure across mainland China using an
771 ensemble algorithm, *Environmental Pollution*, 279, 116932,
772 <https://doi.org/10.1016/j.envpol.2021.116932>, 2021.
- 773 Liu, D., Di, B., Luo, Y., Deng, X., Zhang, H., Yang, F., Grieneisen, M. L., and Zhan, Y.: Estimating
774 ground-level CO concentrations across China based on the national monitoring network and
775 MOPITT: potentially overlooked CO hotspots in the Tibetan Plateau, *Atmospheric Chemistry
776 and Physics*, 19, 12,413–12,430, <https://doi.org/10.5194/acp-19-12413-2019>, 2019.
- 777 Liu, T., Zhou, Y., Wei, J., Chen, Q., Xu, R., Pan, J., Lu, W., Wang, Y., Fan, Z., Li, Y., Xu, L., Cui,
778 X., Shi, C., Zhang, L., Chen, X., Bao, W., Sun, H., and Liu, Y.: Association between short-term
779 exposure to ambient air pollution and dementia mortality in Chinese adults, *Science of The
780 Total Environment*, 849, 157860, <https://doi.org/10.1016/j.scitotenv.2022.157860>, 2022.
- 781 [Liu, W., Wei, J., Cai, M., Qian, Z., Long, Z., Wang, L., Vaughn, M. G., Aaron, H. E., Tong, X., Li,
782 Y., Yin, P., Lin, H., and Zhou, M.: Particulate matter pollution and asthma mortality in China: a
783 nationwide time-stratified case-crossover study from 2015 to 2020, *Chemosphere*, 308,
784 136316, <https://doi.org/10.1016/j.chemosphere.2022.136316>, 2022.](#)
- 785 Ma, Z., Dey, S., Christopher, S., Liu, R., Bi, J., Balyan, P., and Liu, Y.: A review of statistical
786 methods used for developing large-scale and long-term PM_{2.5} models from satellite data,
787 *Remote Sensing of Environment*, 269, 112827, <https://doi.org/10.1016/j.rse.2021.112827>,
788 2022.
- 789 [Maji, K. J. and Sarkar, C.: Spatio-temporal variations and trends of major air pollutants in China
790 during 2015–2018, *Environmental Science and Pollution Research*, 27, 33,792-33,808,
791 <https://doi.org/10.1007/s11356-020-09646-8>, 2020.](#)
- 792 [MEE: Technical regulation for selection of ambient air quality monitoring stations \(on trial\) \(in
793 Chinese\), Ministry of Ecology and Environment of the People’s Republic of China, available
794 at:
795 <https://www.mee.gov.cn/ywgz/fgbz/bz/bzwb/jcffbz/201309/W020131105548727856307.pdf>,
796 2013a.](#)
- 797 [MEE: Specifications and test procedures for ambient air quality continuous automated monitoring](#)

798 [system for SO₂, NO₂, O₃ and CO \(HJ 654-2013\) \(in Chinese\), Ministry of Ecology and](#)
799 [Environment of the People's Republic of China, available at:](#)
800 [https://www.mee.gov.cn/ywgz/fgbz/bz/bzwb/jcffbz/201308/t20130802_20256853.shtml,](https://www.mee.gov.cn/ywgz/fgbz/bz/bzwb/jcffbz/201308/t20130802_20256853.shtml)
801 [2013b.](#)

802 [MEE: Technical specifications for installation and acceptance of ambient air quality continuous](#)
803 [automated monitoring system for SO₂, NO₂, O₃ and CO \(HJ 193-2013\) \(in English\), Ministry](#)
804 [of Ecology and Environment of the People's Republic of China,](#)
805 [https://english.mee.gov.cn/Resources/standards/Air_Environment/air_method/201308/t201308](https://english.mee.gov.cn/Resources/standards/Air_Environment/air_method/201308/t20130816_257560.shtml)
806 [16_257560.shtml, 2013c.](#)

807 MEE: Revision of the ambient air quality standards (GB 3095-2012) (in Chinese), Ministry of
808 Ecology and Environment of the People's Republic of China, available at:
809 http://www.mee.gov.cn/xxgk2018/xxgk/xxgk2001/201808/t20180815_20629602.html, 2018a.

810 [MEE: Technical specifications for operation and quality control of ambient air quality continuous](#)
811 [automated monitoring system for SO₂, NO₂, O₃ and CO \(HJ 818-2018\) \(in Chinese\), Ministry](#)
812 [of Ecology and Environment of the People's Republic of China, available at:](#)
813 http://www.cnemc.cn/jcgf/dqhj/202009/t20200922_20799646.shtml, 2018b.

814 Muñoz-Sabater, J., Dutra, E., Agustí-Panareda, A., Albergel, C., Arduini, G., Balsamo, G.,
815 Boussetta, S., Choulga, M., Harrigan, S., Hersbach, H., Martens, B., Miralles, D. G., Piles, M.,
816 Rodríguez-Fernández, N. J., Zsoter, E., Buontempo, C., and Thépaut, J. N.: ERA5-Land: a
817 state-of-the-art global reanalysis dataset for land applications, *Earth System Science Data*, 13,
818 4349–4383, <https://doi.org/10.5194/essd-13-4349-2021>, 2021.

819 Murray, C. J. L., Aravkin, A. Y., Zheng, P., and Coauthors: Global burden of 87 risk factors in 204
820 countries and territories, 1990–2019: a systematic analysis for the Global Burden of Disease
821 Study 2019, *The Lancet*, 396, 1223–1249, [https://doi.org/10.1016/S0140-6736\(20\)30752-2](https://doi.org/10.1016/S0140-6736(20)30752-2),
822 2020.

823 Orellano, P., Reynoso, J., Quaranta, N., Bardach, A., and Ciapponi, A.: Short-term exposure to
824 particulate matter (PM₁₀ and PM_{2.5}), nitrogen dioxide (NO₂), and ozone (O₃) and all-cause and
825 cause-specific mortality: systematic review and meta-analysis, *Environment International*, 142,
826 105876, <https://doi.org/10.1016/j.envint.2020.105876>, 2020.

827 Qin, K., Rao, L., Xu, J., Bai, Y., Zou, J., Hao, N., Li, S., and Yu, C.: Estimating ground level NO₂
828 concentrations over central-eastern China using a satellite-based geographically and
829 temporally weighted regression model, *Remote Sensing*, 9, 950,
830 <https://doi.org/10.3390/rs9090950>, 2017.

831 Rodriguez, J. D., Perez, A., and Lozano, J. A.: Sensitivity analysis of k-fold cross validation in
832 prediction error estimation, *IEEE Transactions on Pattern Analysis and Machine Intelligence*,
833 32, 569–575, <https://doi.org/10.1109/TPAMI.2009.187>, 2010.

834 [Seo, J., Kim, J. Y., Youn, D., Lee, J. Y., Kim, H., Lim, Y. B., Kim, Y., and Jin, H. C.: On the](#)
835 [multiday haze in the Asian continental outflow: the important role of synoptic conditions](#)
836 [combined with regional and local sources, *Atmospheric Chemistry and Physics*, 17, 9311–](#)
837 [9332, <https://doi.org/10.5194/acp-17-9311-2017>, 2017.](#)

838 [Shah, V., Jacob, D. J., Li, K., Silvern, R. F., Zhai, S., Liu, M., Lin, J., and Zhang, Q.: Effect of](#)
839 [changing NO_x lifetime on the seasonality and long-term trends of satellite-observed](#)
840 [tropospheric NO₂ columns over China, *Atmospheric Chemistry and Physics*, 20, 1483–1495,](#)
841 <https://doi.org/10.5194/acp-20-1483-2020>, 2020.

- 842 Song, J., Du, P., Yi, W., Wei, J., Fang, J., Pan, R., Zhao, F., Zhang, Y., Xu, Z., Sun, Q., Liu, Y.,
843 Chen, C., Cheng, J., Lu, Y., Li, T., Su, H., and Shi, X.: Using an exposome-wide approach to
844 explore the impact of urban environments on blood pressure among adults in Beijing–Tianjin–
845 Hebei and surrounding areas of China, *Environmental Science & Technology*, 56, 8395–8405,
846 <https://doi.org/10.1021/acs.est.1c08327>, 2022.
- 847 [Su, T., Li, Z., Zheng, Y., Luan, Q., and Guo, J.: Abnormally shallow boundary layer associated with](#)
848 [severe air pollution during the COVID-19 lockdown in China, *Geophysical Research Letters*,](#)
849 [47, e2020GL090041, <https://doi.org/10.1029/2020GL090041>, 2020.](#)
- 850 Su, X., Zhang, S., Lin, Q., Wu, Y., Yang, Y., Yu, H., Huang, S., Luo, W., Wang, X., Lin, H., Ma, L.,
851 and Zhang, Z.: Prenatal exposure to air pollution and neurodevelopmental delay in children: a
852 birth cohort study in Foshan, China, *Science of The Total Environment*, 816, 151658,
853 <https://doi.org/10.1016/j.scitotenv.2021.151658>, 2022.
- 854 Sun, Q., Hong, X., and Wold, L. E.: Cardiovascular effects of ambient particulate air pollution
855 exposure, 121, 2755–2765, <https://doi.org/10.1161/CIRCULATIONAHA.109.893461>, 2010.
- 856 Tian, H., Liu, Y., Li, Y., Wu, C.-H., Chen, B., Kraemer, M. U. G., Li, B., Cai, J., Xu, B., Yang, Q.,
857 Wang, B., Yang, P., Cui, Y., Song, Y., Zheng, P., Wang, Q., Bjornstad, O. N., Yang, R.,
858 Grenfell, B. T., Pybus, O. G., and Dye, C.: An investigation of transmission control measures
859 during the first 50 days of the COVID-19 epidemic in China, *Science*, 368, 638–642,
860 <https://doi.org/10.1126/science.abb6105>, 2020.
- 861 [van der A, R. J., Mijling, B., Ding, J., Koukouli, M. E., Liu, F., Li, Q., Mao, H., and Theys, N.:](#)
862 [Cleaning up the air: effectiveness of air quality policy for SO₂ and NO_x emissions in China,](#)
863 [*Atmospheric Chemistry and Physics*, 17, 1775–1789, \[https://doi.org/10.5194/acp-17-1775-\]\(https://doi.org/10.5194/acp-17-1775-2017\)](#)
864 [2017, 2017.](#)
- 865 [Wan, J., Qin, C., Wang, Q., Xiao, Y., Niu, R., Li, X., and Su, J.: A brief overview of the 13th Five-](#)
866 [Year Plan for the protection of ecological environment, in: *Environmental Strategy and*](#)
867 [Planning in China, edited by: Wang, J., Wang, X., and Wan, J., Springer Singapore, Singapore,](#)
868 [57–85, \[https://doi.org/10.1007/978-981-16-6909-5_3\]\(https://doi.org/10.1007/978-981-16-6909-5_3\), 2022.](#)
- 869 Wang, L., Zhang, J., Wei, J., Zong, J., Lu, C., Du, Y., and Wang, Q.: Association of ambient air
870 pollution exposure and its variability with subjective sleep quality in China: A multilevel
871 modeling analysis, *Environmental Pollution*, 312, 120020,
872 <https://doi.org/10.1016/j.envpol.2022.120020>, 2022.
- 873 [Wang, R., Xu, R., Wei, J., Liu, T., Ye, Y., Li, Y., Lin, Q., Zhou, Y., Huang, S., Lv, Z., Tian, Q., and](#)
874 [Liu, Y.: Short-term exposure to ambient air pollution and hospital admissions for sequelae of](#)
875 [stroke in Chinese older adults, *GeoHealth*, 6, e2022GH000700,](#)
876 [<https://doi.org/10.1029/2022GH000700>, 2022.](#)
- 877 Wang, S., Su, H., Chen, C., Tao, W., Streets, D. G., Lu, Z., Zheng, B., Carmichael, G. R., Lelieveld,
878 J., Pöschl, U., and Cheng, Y.: Natural gas shortages during the "coal-to-gas" transition in China
879 have caused a large redistribution of air pollution in winter 2017, *Proceedings of the National*
880 *Academy of Sciences*, 117, 31,018–31,025, <https://doi.org/10.1073/pnas.2007513117>, 2020.
- 881 Wang, Y., Yuan, Q., Li, T., Zhu, L., and Zhang, L.: Estimating daily full-coverage near surface O₃,
882 CO, and NO₂ concentrations at a high spatial resolution over China based on S5P-TROPOMI
883 and GEOS-FP, *ISPRS Journal of Photogrammetry and Remote Sensing*, 175, 311–325,
884 <https://doi.org/10.1016/j.isprsjprs.2021.03.018>, 2021.
- 885 [Wang, Y., Ma, Y. F., Eskes, H., Inness, A., Flemming, J., and Brasseur, G. P.: Evaluation of the](#)

- 886 [CAMS global atmospheric trace gas reanalysis 2003–2016 using aircraft campaign](#)
887 [observations, Atmospheric Chemistry and Physics, 20, 4493–4521, 10.5194/acp-20-4493-](#)
888 [2020, 2020.](#)
- 889 [Wang, Y., Luo, S., Wei, J., Yang, Z., Hu, K., Yao, Y., and Zhang, Y.: Ambient NO₂ exposure hinders](#)
890 [long-term survival of Chinese middle-aged and older adults, Science of The Total](#)
891 [Environment, 855, 158784, <https://doi.org/10.1016/j.scitotenv.2022.158784>, 2023.](#)
- 892 Wei, J., Li, Z., Guo, J., Sun, L., Huang, W., Xue, W., Fan, T., and Cribb, M.: Satellite-derived 1-km-
893 resolution PM₁ concentrations from 2014 to 2018 across China, Environmental Science &
894 Technology, 53, 13,265–13,274, <https://doi.org/10.1021/acs.est.9b03258>, 2019.
- 895 Wei, J., Li, Z., Cribb, M., Huang, W., Xue, W., Sun, L., Guo, J., Peng, Y., Li, J., Lyapustin, A., Liu,
896 L., Wu, H., and Song, Y.: Improved 1-km resolution PM_{2.5} estimates across China using
897 enhanced space–time extremely randomized trees, Atmospheric Chemistry and Physics, 20,
898 3273–3289, <https://doi.org/10.5194/acp-20-3273-2020>, 2020.
- 899 Wei, J., Li, Z., Lyapustin, A., Sun, L., Peng, Y., Xue, W., Su, T., and Cribb, M.: Reconstructing 1-
900 km-resolution high-quality PM_{2.5} data records from 2000 to 2018 in China: spatiotemporal
901 variations and policy implications, Remote Sensing of Environment, 252, 112136,
902 <https://doi.org/10.1016/j.rse.2020.112136>, 2021a.
- 903 Wei, J., Li, Z., Xue, W., Sun, L., Fan, T., Liu, L., Su, T., and Cribb, M.: The ChinaHighPM10
904 dataset: generation, validation, and spatiotemporal variations from 2015 to 2019 across China,
905 Environment International, 146, 106290, <https://doi.org/10.1016/j.envint.2020.106290>, 2021b.
- 906 Wei, J., Li, Z., Li, K., Dickerson, R. R., Pinker, R. T., Wang, J., Liu, X., Sun, L., Xue, W., and
907 Cribb, M.: Full-coverage mapping and spatiotemporal variations of ground-level ozone (O₃)
908 pollution from 2013 to 2020 across China, Remote Sensing of Environment, 270, 112775,
909 <https://doi.org/10.1016/j.rse.2021.112775>, 2022a.
- 910 Wei, J., Liu, S., Li, Z., Liu, C., Qin, K., Liu, X., Pinker, R. T., Dickerson, R. R., Lin, J., Boersma, K.,
911 F., Sun, L., Li, R., Xue, W., Cui, Y., Zhang, C., and Wang, J.: Ground-level NO₂ surveillance
912 from space across China for high resolution using interpretable spatiotemporally weighted
913 artificial intelligence, Environmental Science & Technology, 56, 9988–9998,
914 <https://doi.org/10.1021/acs.est.2c03834>, 2022b.
- 915 WHO: Coronavirus Disease (COVID-19) Pandemic, The World Health Organization, available
916 online: <https://www.who.int/emergencies/diseases/novel-coronavirus-2019>, 2020.
- 917 [WHO: WHO global air quality guidelines. Particulate matter \(PM_{2.5} and PM₁₀\), ozone, nitrogen](#)
918 [dioxide, sulfur dioxide and carbon monoxide, Geneva: World Health Organization, Licence:](#)
919 [CC BY-NC-SA 3.0 IGO, Licence: CC BY-NC-SA 3.0 IGO, 2021.](#)
- 920 Wu, H., Zhang, Y., Zhao, M., Liu, W., Magnussen, C. G., Wei, J., and Xi, B.: Short-term effects of
921 exposure to ambient PM₁ on blood pressure in children and adolescents aged 9 to 18 years in
922 Shandong Province, China, Atmospheric Environment, 283, 119180,
923 <https://doi.org/10.1016/j.atmosenv.2022.119180>, 2022a.
- 924 Wu, H., Lu, Z., Wei, J., Zhang, B., Liu, X., Zhao, M., Liu, W., Guo, X., and Xi, B.: Effects of the
925 COVID-19 lockdown on air pollutant levels and associated reductions in ischemic stroke
926 incidence in Shandong Province, China, Frontiers in Public Health, 10,
927 <https://doi.org/10.3389/fpubh.2022.876615>, 2022b.
- 928 [Wu, S., Huang, B., Wang, J., He, L., Wang, Z., Yan, Z., Lao, X., Zhang, F., Liu, R., and Du, Z.:](#)
929 [Spatiotemporal mapping and assessment of daily ground NO₂ concentrations in China using](#)

930 [high-resolution TROPOMI retrievals, *Environmental Pollution*, 273, 116456,](#)
931 <https://doi.org/10.1016/j.envpol.2021.116456>, 2021.

932 [Wu, X., Yang, Y., Gong, Y., Deng, Z., Wang, Y., Wu, W., Zheng, C., and Zhang, Y.: Advances in air](#)
933 [pollution control for key industries in China during the 13th Five-Year Plan, *Journal of*](#)
934 [Environmental Sciences](#), <https://doi.org/10.1016/j.jes.2022.09.008>, 2022.

935 Xu, H., Bechle, M. J., Wang, M., Szpiro, A. A., Vedal, S., Bai, Y., and Marshall, J. D.: National
936 PM_{2.5} and NO₂ exposure models for China based on land use regression, satellite
937 measurements, and universal kriging, *Science of The Total Environment*, 655, 423–433,
938 <https://doi.org/10.1016/j.scitotenv.2018.11.125>, 2019.

939 Xu, J., Zhou, J., Luo, P., Mao, D., Xu, W., Nima, Q., Cui, C., Yang, S., Ao, L., Wu, J., Wei, J., Chen,
940 G., Li, S., Guo, Y., Zhang, J., Liu, Z., and Zhao, X.: Associations of long-term exposure to
941 ambient air pollution and physical activity with insomnia in Chinese adults, *Science of The*
942 *Total Environment*, 792, 148197, <https://doi.org/10.1016/j.scitotenv.2021.148197>, 2021.

943 [Xu, R., Wei, J., Liu, T., Li, Y., Yang, C., Shi, C., Chen, G., Zhou, Y., Sun, H., and Liu, Y.:](#)
944 [Association of short-term exposure to ambient PM₁ with total and cause-specific](#)
945 [cardiovascular disease mortality, *Environment International*, 169, 107519,](#)
946 <https://doi.org/10.1016/j.envint.2022.107519>, 2022a.

947 Xu, R., Shi, C., Wei, J., Lu, W., Li, Y., Liu, T., Wang, Y., Zhou, Y., Chen, G., Sun, H., and Liu, Y.:
948 Cause-specific cardiovascular disease mortality attributable to ambient temperature: a time-
949 stratified case-crossover study in Jiangsu province, China, *Ecotoxicology and Environmental*
950 *Safety*, 236, 113498, <https://doi.org/10.1016/j.ecoenv.2022.113498>, 2022b.

951 Xu, R., Wang, Q., Wei, J., Lu, W., Wang, R., Liu, T., Wang, Y., Fan, Z., Li, Y., Xu, L., Shi, C., Li,
952 G., Chen, G., Zhang, L., Zhou, Y., Liu, Y., and Sun, H.: Association of short-term exposure to
953 ambient air pollution with mortality from ischemic and hemorrhagic stroke, *European Journal*
954 *of Neurology*, 29, 1994–2005, <https://doi.org/10.1111/ene.15343>, 2022c.

955 [Xu, W. Y., Zhao, C. S., Ran, L., Deng, Z. Z., Liu, P. F., Ma, N., Lin, W. L., Xu, X. B., Yan, P., He,](#)
956 [X., Yu, J., Liang, W. D., and Chen, L. L.: Characteristics of pollutants and their correlation to](#)
957 [meteorological conditions at a suburban site in the North China Plain, *Atmospheric Chemistry*](#)
958 [and Physics](#), 11, 4353–4369, <https://doi.org/10.5194/acp-11-4353-2011>, 2011.

959 [Yoo, J.-M., Lee, Y.-R., Kim, D., Jeong, M.-J., Stockwell, W. R., Kundu, P. K., Oh, S.-M., Shin, D.-](#)
960 [B., and Lee, S.-J.: New indices for wet scavenging of air pollutants \(O₃, CO, NO₂, SO₂, and](#)
961 [PM₁₀\) by summertime rain, *Atmospheric Environment*, 82, 226–237,](#)
962 <https://doi.org/10.1016/j.atmosenv.2013.10.022>, 2014.

963 Zhan, Y., Luo, Y., Deng, X., Zhang, K., Zhang, M., Grieneisen, M. L., and Di, B.: Satellite-based
964 estimates of daily NO₂ exposure in China using hybrid random forest and spatiotemporal
965 kriging model, *Environmental Science & Technology*, 52, 4180–4189,
966 <https://doi.org/10.1021/acs.est.7b05669>, 2018.

967 [Zhang, B., Rong, Y., Yong, R., Qin, D., Li, M., Zou, G., and Pan, J.: Deep learning for air pollutant](#)
968 [concentration prediction: a review, *Atmospheric Environment*, 290, 119347,](#)
969 <https://doi.org/10.1016/j.atmosenv.2022.119347>, 2022.

970 [Zhang, C., Liu, C., Hu, Q., Cai, Z., Su, W., Xia, C., Zhu, Y., Wang, S., and Liu, J.: Satellite UV-Vis](#)
971 [spectroscopy: implications for air quality trends and their driving forces in China during 2005–](#)
972 [2017, *Light: Science & Applications*, 8, 100, 10.1038/s41377-019-0210-6](#), 2019.

973 [Zhang, Q., Zheng, Y., Tong, D., Shao, M., Wang, S., Zhang, Y., Xu, X., Wang, J., He, H., Liu, W.,](#)

974 [Ding, Y., Lei, Y., Li, J., Wang, Z., Zhang, X., Wang, Y., Cheng, J., Liu, Y., Shi, Q., Yan, L.,](#)
975 [Geng, G., Hong, C., Li, M., Liu, F., Zheng, B., Cao, J., Ding, A., Gao, J., Fu, Q., Huo, J., Liu,](#)
976 [B., Liu, Z., Yang, F., He, K., and Hao, J.: Drivers of improved PM_{2.5} air quality in China from](#)
977 [2013 to 2017, *Proceedings of the National Academy of Sciences*, 116, 24,463–24,469,](#)
978 <https://doi.org/10.1073/pnas.1907956116>, 2019.

979 Zhang, Y., Li, Z., Wei, J., Zhan, Y., Liu, L., Yang, Z., Zhang, Y., Liu, R., and Ma, Z.: Long-term
980 exposure to ambient NO₂ and adult mortality: a nationwide cohort study in China, *Journal of*
981 *Advanced Research*, 41, 13–22, <https://doi.org/10.1016/j.jare.2022.02.007>, 2022.

982 Zhang, Z., Wang, J., Hart, J. E., Laden, F., Zhao, C., Li, T., Zheng, P., Li, D., Ye, Z., and Chen, K.:
983 National scale spatiotemporal land-use regression model for PM_{2.5}, PM₁₀ and NO₂
984 concentration in China, *Atmospheric Environment*, 192, 48–54,
985 <https://doi.org/10.1016/j.atmosenv.2018.08.046>, 2018.

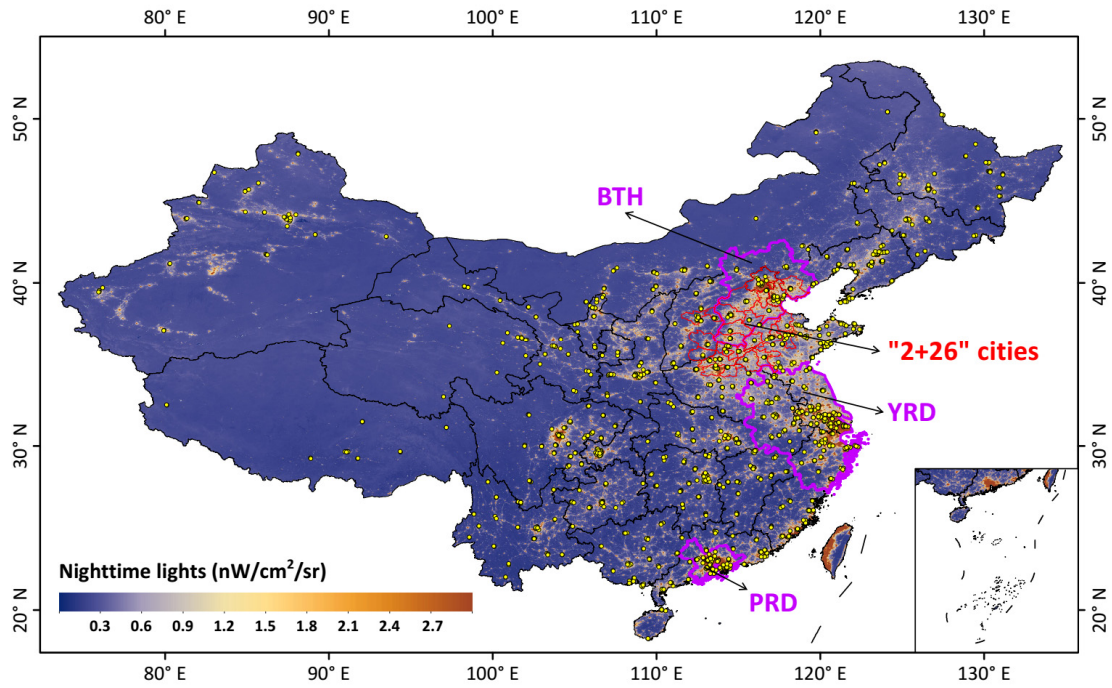
986 [Zheng, B., Chevallier, F., Ciais, P., Yin, Y., Deeter, M. N., Worden, H. M., Wang, Y., Zhang, Q., and](#)
987 [He, K.: Rapid decline in carbon monoxide emissions and export from East Asia between years](#)
988 [2005 and 2016, *Environmental Research Letters*, 13, 044007, https://doi.org/10.1088/1748-](#)
989 [9326/aab2b3](#), 2018.

990 Zheng, B., Zhang, Q., Geng, G., Chen, C., Shi, Q., Cui, M., Lei, Y., and He, K.: Changes in China's
991 anthropogenic emissions and air quality during the COVID-19 pandemic in 2020, *Earth*
992 *System Science Data*, 13, 2895–2907, <https://doi.org/10.5194/essd-13-2895-2021>, 2021.

993
994

995 **Figures**

996



997

998

999

1000

1001

1002

1003

Figure 1. Geographical locations of ground-based stations from the China National Environmental Monitoring Centre network (marked as yellow dots) monitoring gaseous pollutants across China. The background shows the nighttime-light level, an estimate of population. Purple boundaries three typical urban agglomerations: the Beijing-Tianjin-Hebei (BTH) region, the Yangtze River Delta (YRD), and the Pearl River Delta (PRD).

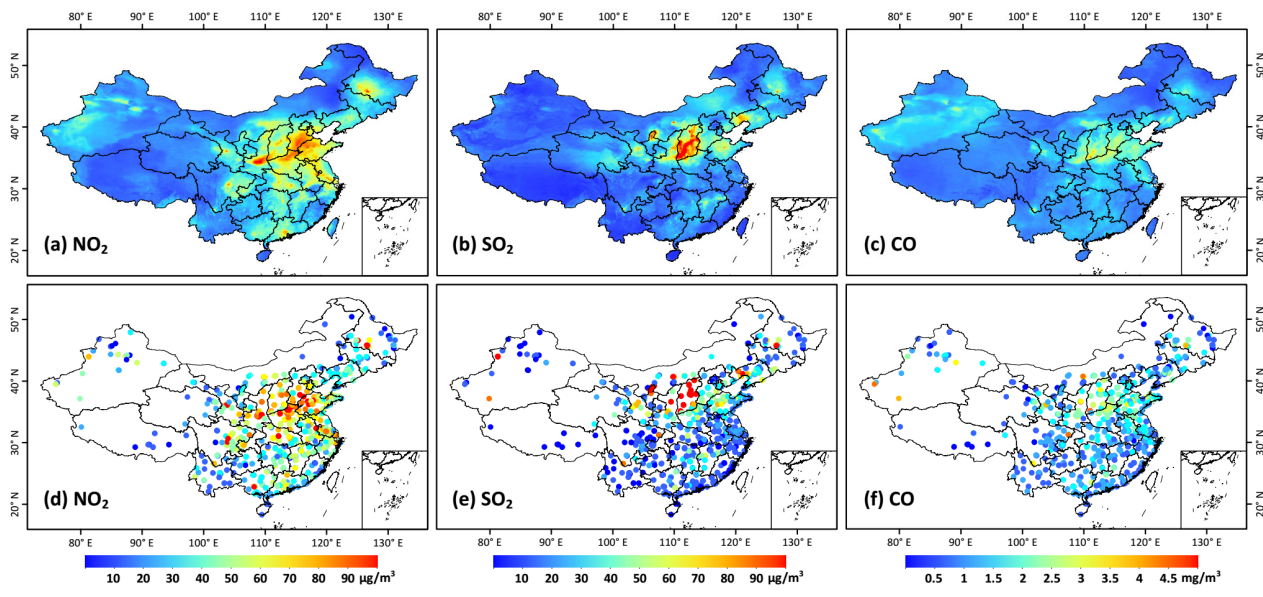
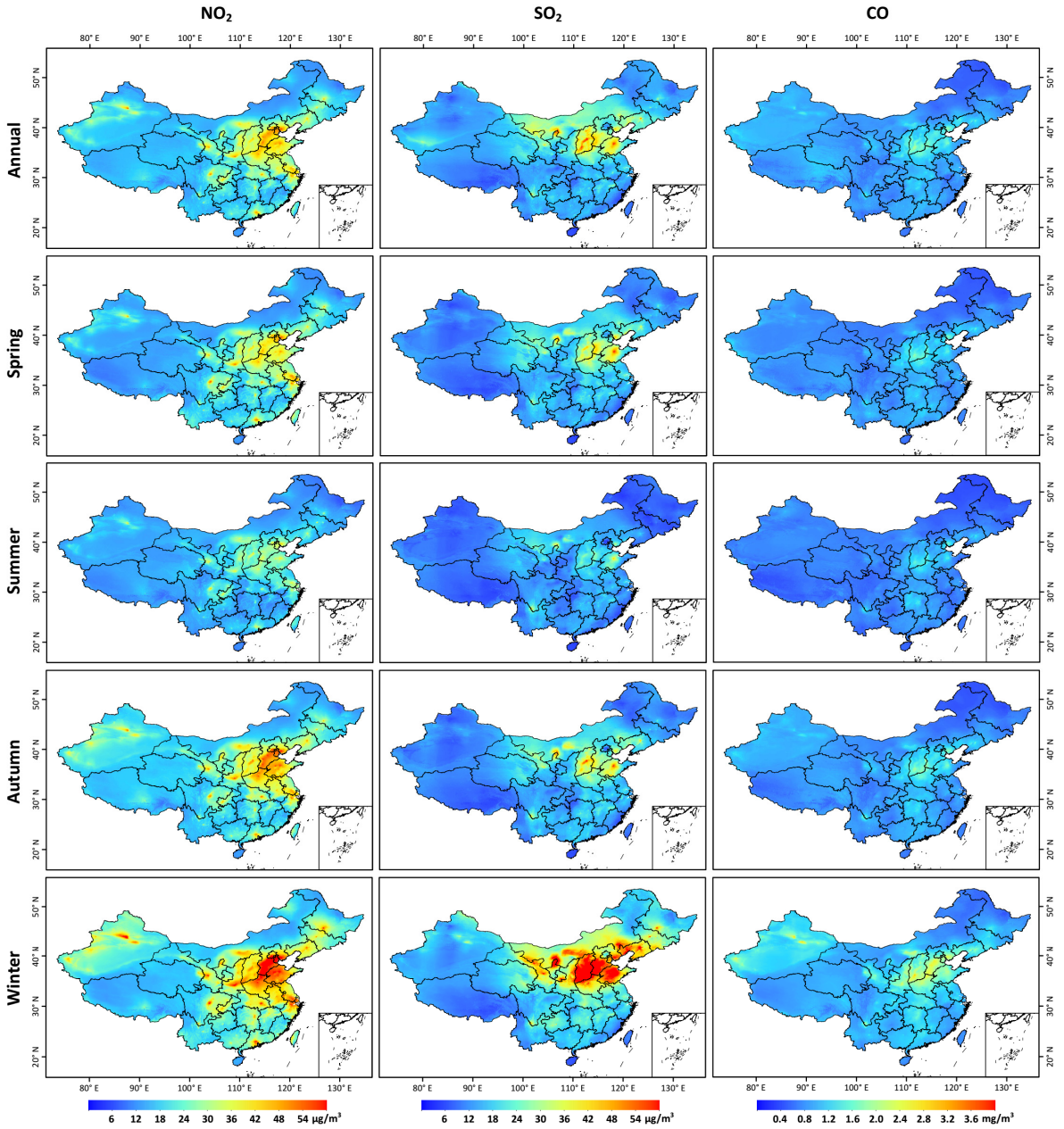


Figure 2. A typical example of (a-c) big-data-derived (horizontal resolution = 10 km) seamless surface NO₂ (µg/m³), SO₂ (µg/m³), and CO (mg/m³) concentrations and (d-f) corresponding ground measurements on 1 January 2018 in China.

1004
1005
1006
1007

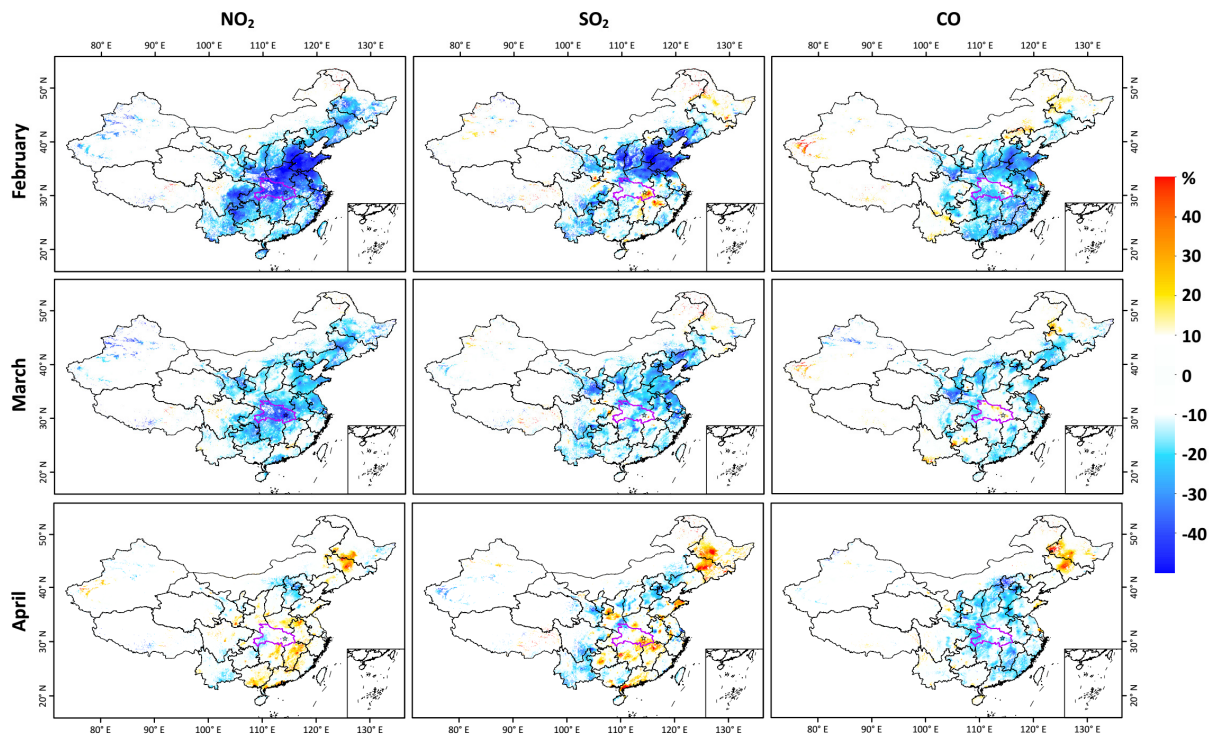


1008

1009

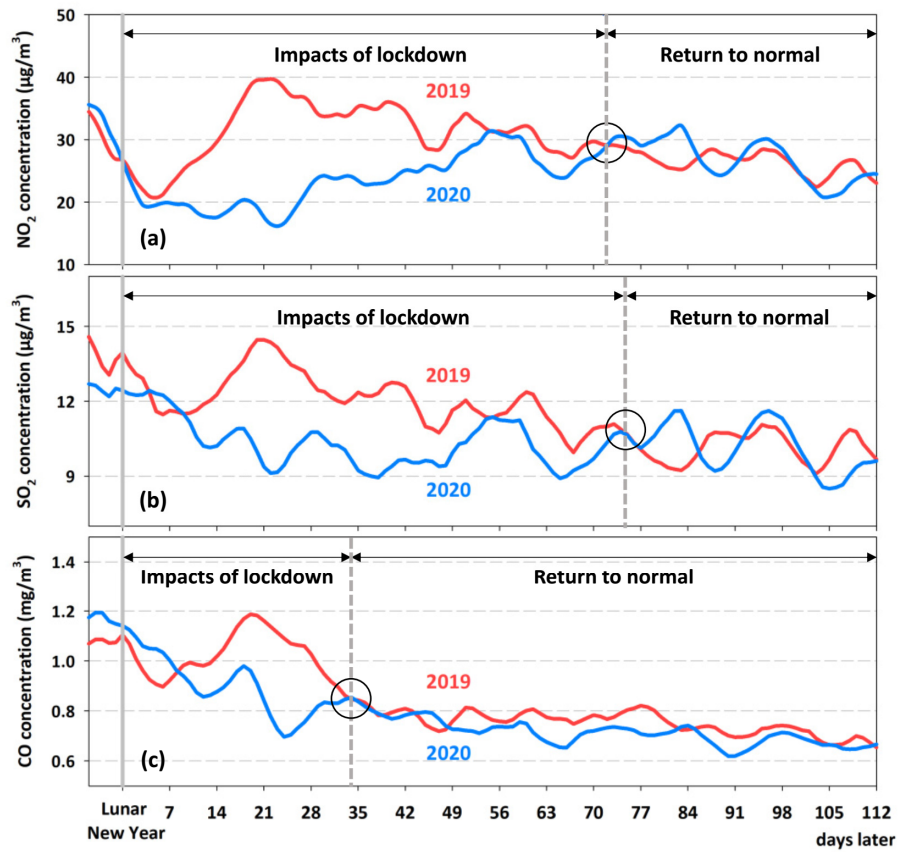
1010

Figure 3. Annual and seasonal mean maps (horizontal resolution = 10 km) of surface NO_2 ($\mu\text{g}/\text{m}^3$), SO_2 ($\mu\text{g}/\text{m}^3$), and CO (mg/m^3) averaged over the period 2013–2020 in China.



1011
 1012
 1013
 1014
 1015

Figure 4. Relative changes (%) in surface NO₂, SO₂, and CO concentrations in February, March, and April between 2019 and 2020 in populated areas of China. The area outlined in magenta and the star in each panel indicate Hubei Province and Wuhan City, respectively.



1016
 1017
 1018
 1019
 1020
 1021
 1022

Figure 5. Time series of the seven-day moving averages of daily population-weighted surface (a) NO₂, (b) SO₂, and (c) CO concentrations after the Lunar New Year of 2019 and 2020 in China. The black circle in each panel shows the turning point when the gaseous pollutants began to return to their normal levels.

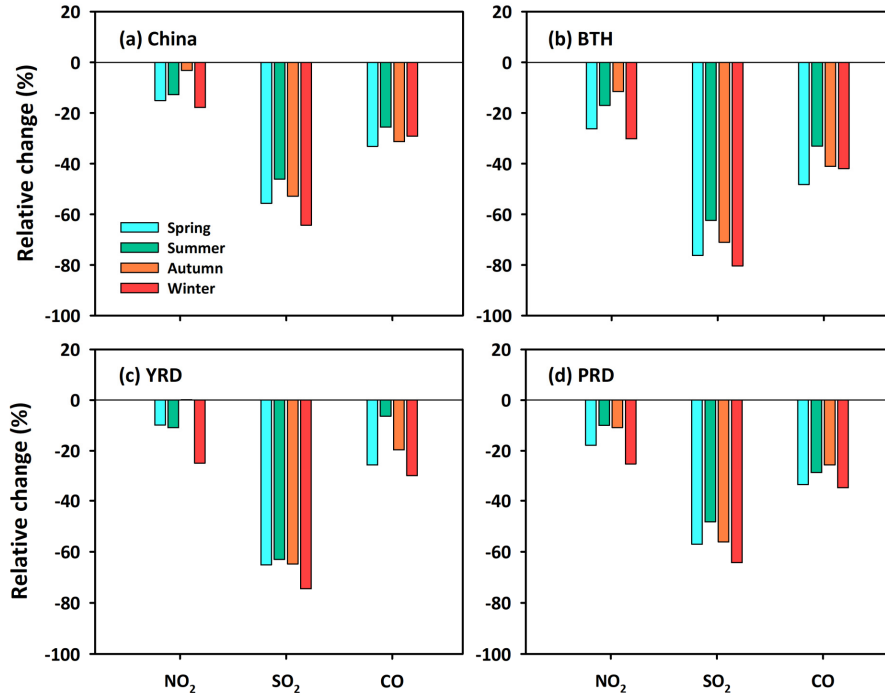


Figure 6. Relative changes (%) in seasonal mean surface NO₂, SO₂, and CO concentrations between 2013 and 2020 over (a) China, (b) the Beijing-Tianjin-Hebei (BTH) region, (c) the Yangtze River Delta (YRD), and (d) the Pearl River Delta (PRD).

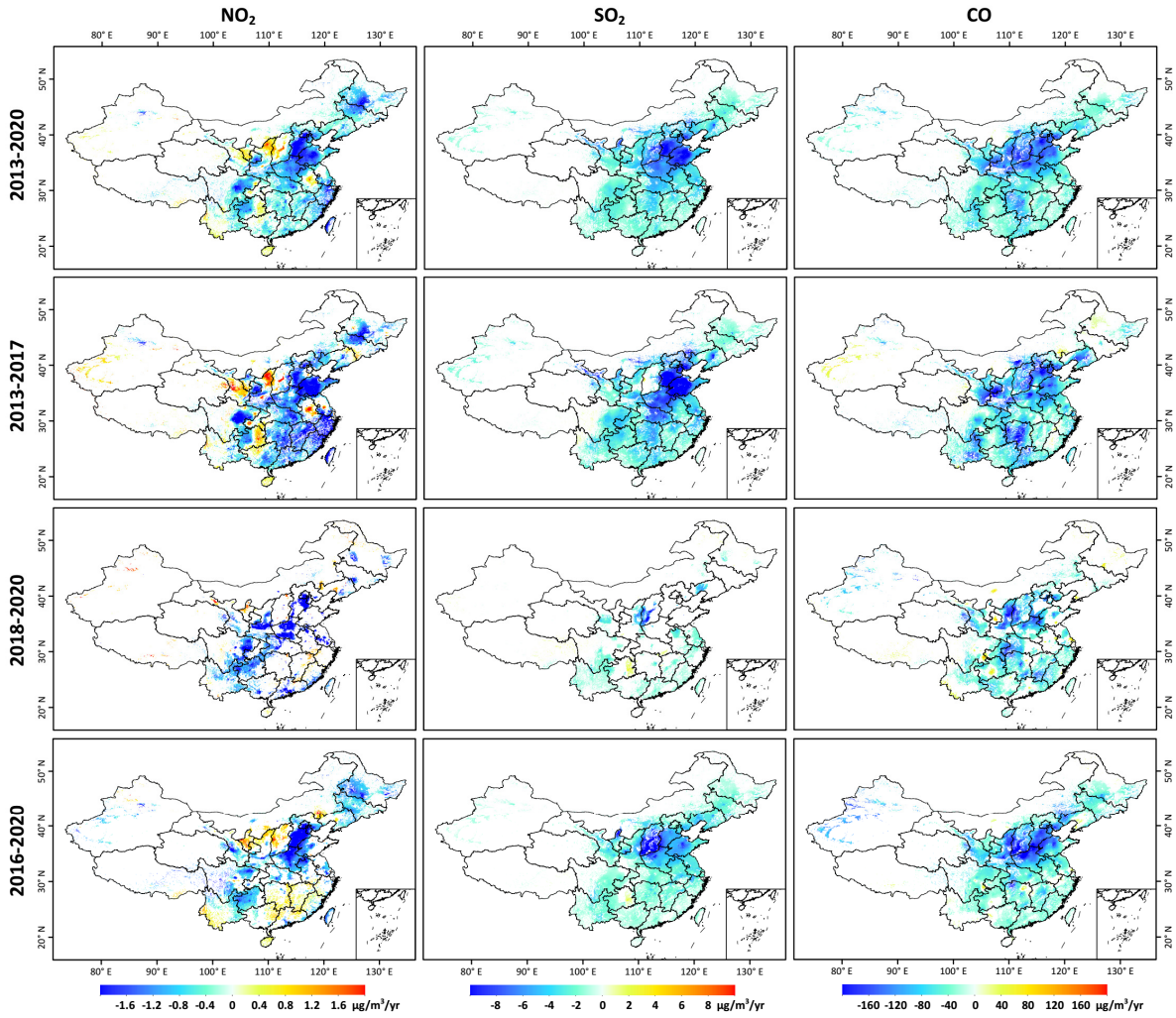
1023

1024

1025

1026

1027



1028

1029

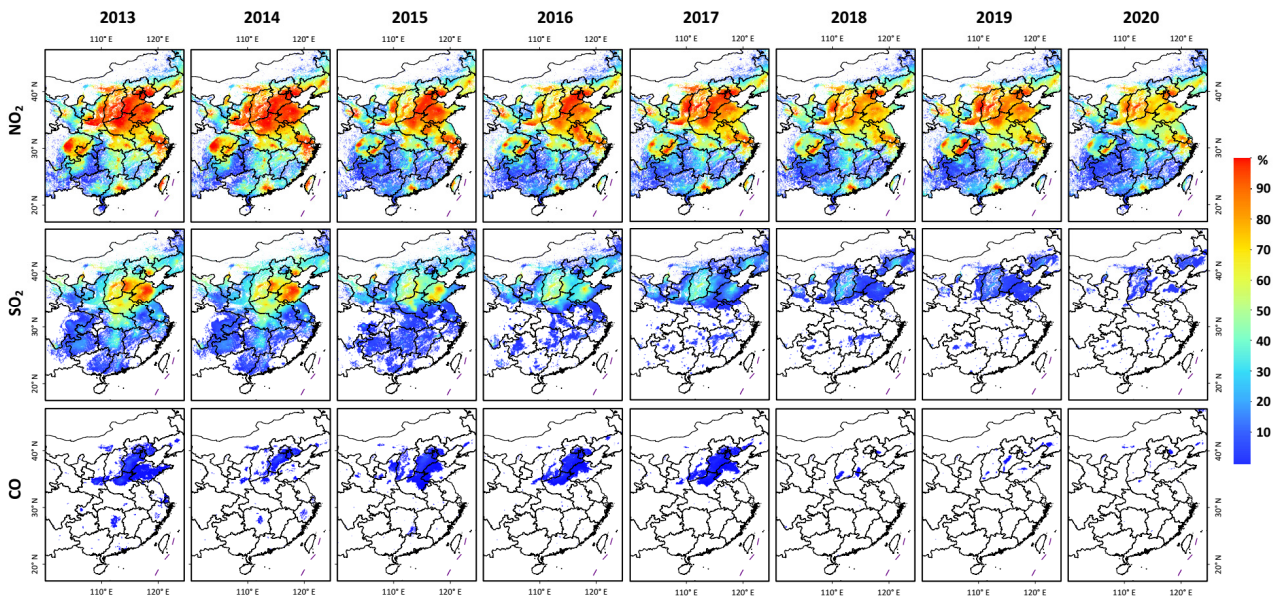
1030

1031

1032

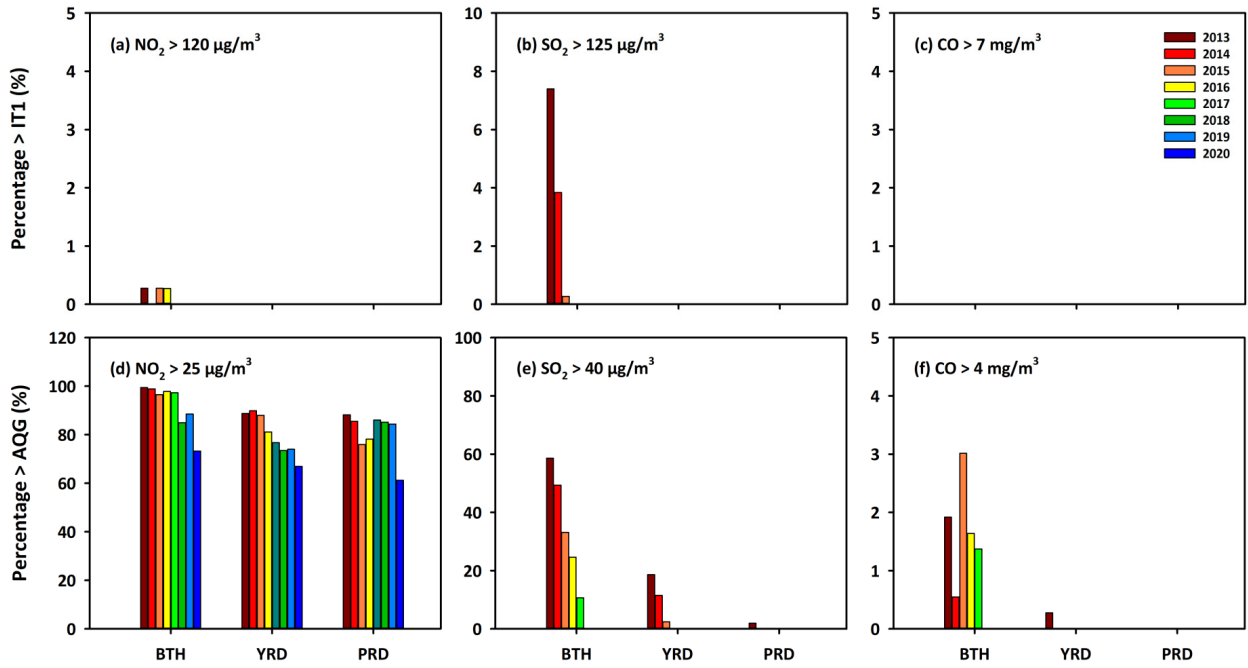
1033

Figure 7. Temporal trends of surface NO₂, SO₂, and CO concentrations during the whole period (2013–2020), the Clean Air Action Plan (2013–2017), the Blue Sky Defense War (2018–2020), and the 13rd Five-Year Plan (2016–2020) in China. Only regions with trends that are significant at the 95% ($p < 0.05$) confidence level are shown.



1034
 1035
 1036
 1037
 1038
 1039

Figure 8. Spatial distributions of the percentage of days exceeding the WHO recommended short-term desired air quality guidelines level for surface NO₂ (daily mean > 25 μg/m³), SO₂ (daily mean > 40 μg/m³), and CO (daily mean > 4 mg/m³) for each year from 2013 to 2020 in populated areas in eastern China.



1040
1041
1042
1043
1044
1045

Figure 9. Percentage of days (%) exceeding the WHO recommended short-term (a-c) minimum interim target (IT1) and (d-f) desired air quality guidelines (AQG) level for surface NO_2 , SO_2 , and CO for each year from 2013 to 2020 in three typical urban agglomerations: the Beijing-Tianjin-Hebei (BTH) region, the Yangtze River Delta (YRD), and the Pearl River Delta (PRD).

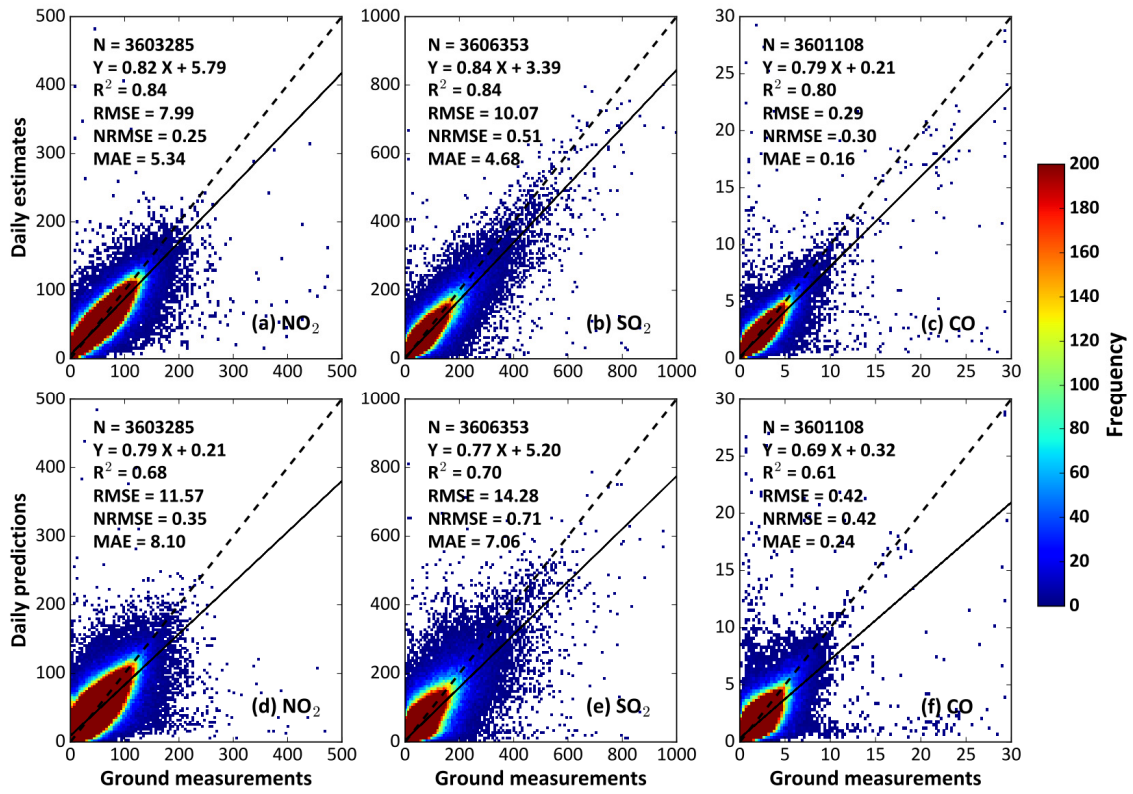
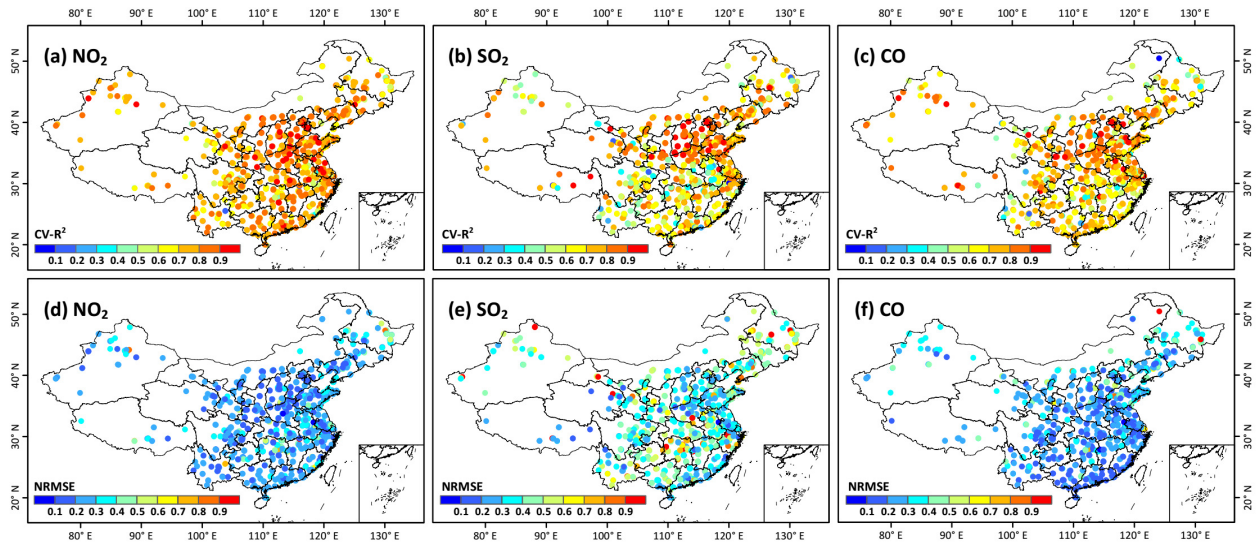


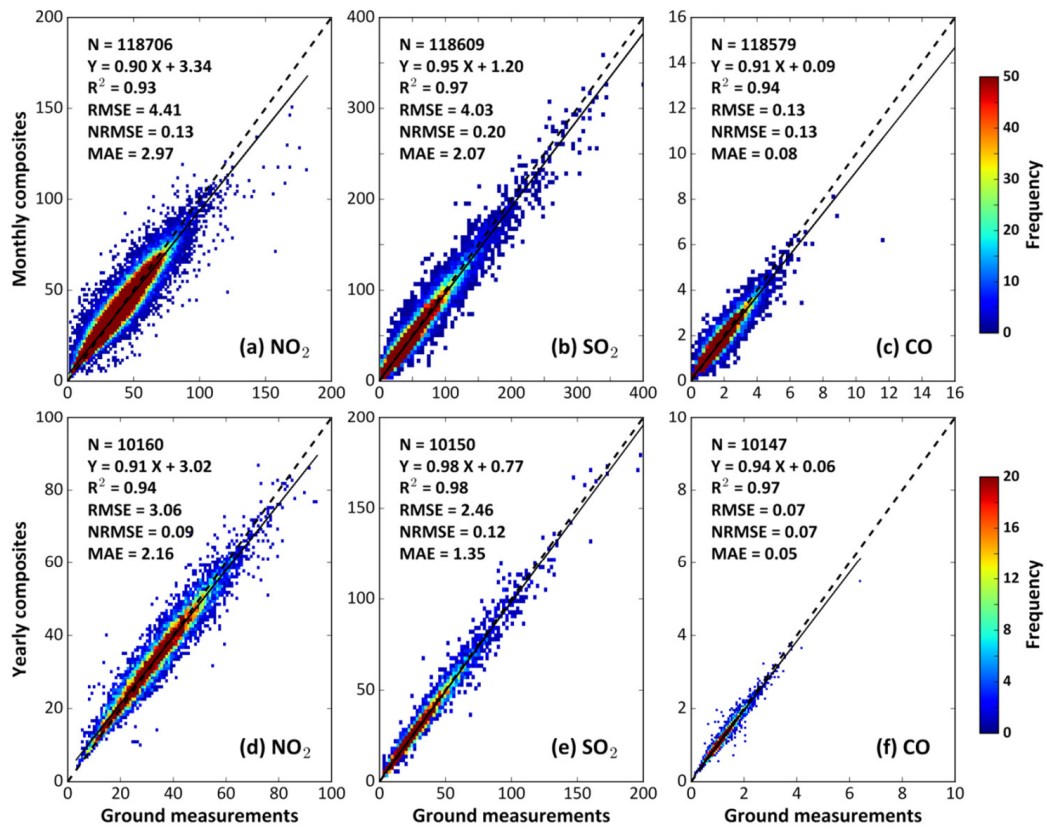
Figure 10. Density plots of daily (a-c) estimates and (d-f) predictions of ground-level NO₂ (μg/m³), SO₂ (μg/m³), and CO (mg/m³) concentrations as a function of ground measurements in China from 2013 to 2020 using the out-of-sample (top panels) and out-of-station (bottom panels) cross-validation methods.

1046
1047
1048
1049
1050
1051



1052
 1053
 1054
 1055
 1056

Figure 11. Sample-based spatial validation of daily ground-level ~~three~~ NO_2 ($\mu\text{g}/\text{m}^3$), SO_2 ($\mu\text{g}/\text{m}^3$), and CO (mg/m^3) estimates at each individual monitoring station in China from 2013 to 2020: (a-c) accuracy (i.e., CV-R^2) and (d-f) uncertainty (i.e., RMSE/NRMSE).



1057
1058 **Figure 12. Sample-based temporal validation** of (a-c) monthly and (d-f) yearly composites of
1059 ground-level NO₂ (μg/m³), SO₂ (μg/m³), and CO (mg/m³) against as a function of ground
1060 measurements from 2013 to 2020 in China.
1061

1062 **Tables**

1063

1064 **Table 1.** Statistics of the overall accuracies and predictive abilities of ambient gaseous pollutants for
1065 each year in China from 2013 to 2020.

Year	Sample size N (10 ³)	Overall accuracy						Predictive ability					
		NO ₂		SO ₂		CO		NO ₂		SO ₂		CO	
		R ²	RMSE	R ²	RMSE	R ²	RMSE	R ²	RMSE	R ²	RMSE	R ²	RMSE
2013	169	0.77	12.48	0.83	17.97	0.80	0.56	0.53	18.16	0.68	25.04	0.60	0.78
2014	324	0.76	10.97	0.83	15.87	0.77	0.38	0.54	15.56	0.66	22.45	0.51	0.57
2015	518	0.79	9.34	0.80	13.71	0.74	0.38	0.61	13.10	0.61	19.49	0.50	0.55
2016	516	0.82	8.59	0.83	11.26	0.76	0.34	0.64	12.20	0.65	16.28	0.57	0.46
2017	527	0.86	7.57	0.86	7.79	0.82	0.24	0.72	10.67	0.74	10.80	0.70	0.32
2018	513	0.87	6.92	0.83	5.61	0.82	0.20	0.76	9.33	0.68	7.80	0.69	0.26
2019	515	0.87	6.78	0.81	4.84	0.82	0.20	0.77	9.23	0.66	6.63	0.70	0.25
2020	522	0.89	5.78	0.80	4.02	0.82	0.17	0.79	8.04	0.62	5.57	0.69	0.23

1066

1067
1068

Table 2. Comparison of long-term datasets of different gaseous pollutants focusing on the whole of China.

Species	Model	Missing values	Spatial resolution	Main input	Validation period	CV-R ²	RMSE	Literature
NO ₂	RF-STK	Yes	0.25°	OMI	2013–2016	0.62	13.3	(Zhan et al., 2018)
	RF-K	Yes	0.25°	OMI	2013–2018	0.64	11.4	(Dou et al., 2021)
	KCS	Yes	0.125°	OMI	2014–2016	0.72	7.9	(Z.-Y. Chen et al., 2019)
	LUR	Yes	0.125°	OMI	2014–2015	0.78	-	(H. Xu et al., 2019)
	LME	Yes	0.1°	OMI	2014–2020	0.65	7.9	(Chi et al., 2021)
	XGBoost	Yes	0.125°	TROPOMI	2018–2020	0.67	6.4	(Chi et al., 2022)
	XGBoost	Yes	0.05°	TROPOMI	2018–2019	0.83	7.6	(Liu, 2021)
	LightGBM	No	0.05°	TROPOMI	2018–2020	0.83	6.6	(Y. Wang et al., 2021)
	SWDF	No	0.01°	TROPOMI	2019–2020	0.93	4.9	(Wei et al., 2022b)
STET	No	0.1°	Big data	2013–2020	0.84	8.0	This study	
SO ₂	RF	No	0.25°	Emissions	2013–2014	0.64	17.1	(R. Li et al., 2020)
	STET	No	0.1	Big data	2013–2020	0.84	10.1	This study
CO	RF-STK	Yes	0.1	MOPITT	2013–2016	0.51	0.54	(D. Liu et al., 2019)
	LightGBM	No	0.07°	TROPOMI	2018–2020	0.71	0.26	(Y. Wang et al., 2021)
	STET	No	0.1°	Big data	2013–2020	0.80	0.29	This study

1069 KCS: kriging-calibrated satellite method; LightGBM: light gradient boosted model; LME: linear mixed effect model;
 1070 LUR: land use regression; MOPITT: Measurements of Pollution in the Troposphere; OMI: Ozone Monitoring
 1071 Instrument; RF: random forest; RF-K: random forest integrated with K-means; RF-STK: random-forest-spatiotemporal-
 1072 kriging model; STET: space-time extremely randomized tree; SWDF: spatiotemporally weighted deep forest;
 1073 TROPOMI: TROPospheric Monitoring Instrument; XGBoost: extreme gradient boosting